Corn yield, water productivity, and soil hydraulics under deficit irrigation with biochar and APSA-80 in Southwest Kansas

by

Msgina Aregawi

B.S., Mattu University, 2019

A THESIS

submitted in partial fulfillment of the requirements for the degree

MASTER OF SCIENCE

Carl and Melinda Helwig Department of Agricultural and Biological Engineering
Carl R. Ice College of Engineering

KANSAS STATE UNIVERSITY
Manhattan, Kansas

2026

Approved by:

Co-Major Professor
Dr. Jonathan Aguilar

Approved by:

Co-Major Professor
Dr. Vaishali Sharda

Copyright

© Msgina Aregawi 2026.

Abstract

The increasing rate of groundwater extraction from the Ogallala Aquifer, combined with lithologic and statutory limitations imposes possible reduction of water use by corn producers irrigating in southwest Kansas. During the cropping season of 2025, this field study analyzed the effects of deficit irrigation (W100 (203.2 mm) and W50 (101.6 mm)) as well as IBI-certified granular softwood biochar (0, 1, and 3.5 t ha^{-1}) and APSA-80 non-ionic soil surfactant (presence/absence) on corn grain yield, irrigation water productivity (IWP), and soil hydraulic parameters in a research experiment on the soils of Southwest Research-Extension Center (SWREC), Garden City, Finney County, Kansas. The design of the experiment involved a balanced split-plot RCBD design with three replications (n=36 subplots) of Ulysses silt loam soil in a no-till system. Irrigation was the whole-plot variable, and biochar and APSA-80 were subplot variables. Pre- and post-treatment field-saturated hydraulic conductivity (K_{fs}) was measured using a SATURO dual-head infiltrometer, and volumetric water content (VWC) at 10 cm depth was measured at four growth stages using Acclima TDR probes. The total seasonal precipitation was 284.2 mm, 115.1 mm of which fell after September.

W50 irrigation produced a yield loss of only 7.1% (12,011.67 kg ha^{-1} vs. 12,925.60 kg ha^{-1}; $F_{1,2} = 8.904$, $p = 0.0964$, †). On the other hand, IWP increased by 85.9% (118.22 vs. 63.61 kg ha^{-1} mm^{-1}; $F_{1,2} = 606.31$, $p = 0.0016$, **). This demonstrates the economic and agronomic advantages of deficit irrigation under the constraint of Ogallala allocation. The yield loss was shown to have the same trend in all three blocks, but because of the conservative character of the test with df = 2, significance was not achieved at $\alpha = 0.05$. Neither biochar nor APSA-80 demonstrated a significant main effect on any response variable. There was a marginal interaction between irrigation and APSA-80 ($F_{1,20} = 3.997$, $p = 0.0593$, †), which buffers the K_{fs} reduction in the case of W100 irrigation (fold change: 0.921 vs 0.809), whereas there was no effect on W50 irrigation (0.867 vs

0.883) because of the higher hydraulic loading in the case of W100 irrigation. K_{fs} decreased in 34 of 36 subplots (average fold change = 0.870) but proved to be insignificant in predicting the yield (ρ = +0.048, NS). The K_{fs} reduction did not translate into yield penalty under the linear move overhead irrigation system used in this study; pre-irrigation VWC (ρ = +0.377, p = 0.023, *) and VWC at harvest (ρ = +0.338, p = 0.044, *) showed significant relationships with yield. This suggests that between-event root zone water storage is the major predictor of yield variability.

Keywords: *deficit irrigation; irrigation water productivity; soil surfactant; biochar; volumetric water content; Ogallala aquifer; split-plot RCBD; semi-arid High Plains; field saturated hydraulic conductivity; APSA-80.*

Table of Contents

List of Figures ix
List of Tables x
Acknowledgements xii
Dedication xiii
Chapter 1 - Introduction 1
1.1 Background and Problem Statement 1
1.2 Deficit Irrigation as a Water Conservation Strategy 3
1.3 Soil Hydraulic Function and Its Role in Irrigation Performance 4
1.4 Soil Amendments: Biochar and APSA-80 5
1.5 Study Motivation and Significance 6
1.6 Research Objectives 7
1.7 Research Hypotheses 8
1.8 Thesis Organization 9
Chapter 2-Literature Review 1
2.1 Semi-Arid Irrigated Agriculture in Southwest Kansas 1
2.2 High Plains Aquifer Depletion and Irrigation Sustainability 2
2.2.1 Climate Change as a Compounding Driver of Irrigation Demand 3
2.3 Deficit Irrigation: Definitions, Approaches, and Trade-offs with Yields 4
2.4 Water Productivity Metrics in Irrigated Corn Production 5
2.4.1 Irrigation Water Productivity vs. Total Water Productivity 5
2.4.2 Typical IWP Values for Irrigated Corn in the High Plains 6
2.5 Soil Hydraulic Function and Irrigation Performance 7
2.5.1 Field-Saturated Hydraulic Conductivity (K_{fs}) 7
2.5.2 Volumetric Water Content Dynamics and Irrigation Interpretation 7
2.6 Biochar: Properties, Hydraulic Effects, and Amendment Considerations 8
2.6.1 Biochar Characterization and Soil Carbon Sequestration 8
2.6.2 Biochar Effects on Soil Hydraulic Properties 9
2.6.3 Biochar and Crop Yield 10

2.6.4 Biochar Application Methods, Wind Displacement, and Cost Considerations 12
2.7 APSA-80: Surfactant Properties and Soil Hydraulic Redistribution 13
2.7.1 Biological Surfactants: Bacillus-Derived Surfactin as a Natural Analog to Synthetic Soil Surfactants 15
2.8 Relationships Between Soil Hydraulic Function and Crop Outcomes Under Deficit Irrigation 16
2.9 Research Gaps Addressed by This Study 17
2.10 Conceptual Framework and Literature Summary 17
Chapter 3 - Materials and Methods 20
3.1 Study Site and Soil Characterization 20
3.2 Experimental Design 22
3.3 Corn Production and Agronomic Management 23
3.4 Biochar Amendment Characteristics and Application 24
3.5 APSA-80 Application 26
3.6 Irrigation Management and Scheduling 26
3.7 Field-Saturated Hydraulic Conductivity (K_{fs}) Measurement 28
3.8 Volumetric Water Content (VWC) Monitoring 29
3.9 Irrigation Water Productivity (IWP) and Total Water Productivity (TWP) 30
3.10 Climate and Evapotranspiration Data 30
3.11 Statistical Analysis 31
Chapter 4 - Results 33
4.1 Statistical Reporting Framework 33
4.2 Growing Season Climate and Water Budget 34
4.2.1 Seasonal Precipitation and Evapotranspiration 34
4.2.2 Water Budget for Irrigation Treatments 35
4.3 Response of corn grain yield to irrigation and amendment treatments 35
4.3.1 Influence of irrigation on yield 36
4.3.2 Yield Response to Amendments 37
4.4 Irrigation Water Productivity and Total Water Productivity 39
4.5 Field-Saturated Hydraulic Conductivity (K_{fs}) 40
4.5.1 Pre-Treatment Baseline Equivalence 40

4.5.2 APSA-80 Effects on K_{fs}: Irrigation Interaction 41
4.6 Volumetric Water Content Dynamics 43
4.6.1 Baseline and Post-Irrigation VWC 43
4.6.2 Pre-Irrigation Trough VWC and Between-Event Depletion 44
4.7 Correlations Between Soil Hydraulics and Grain Yield 47
4.8 Summary of Major Results 49
Chapter 5 - Discussion, Conclusion, and Implications 50
5.1 Yield Response to Deficit Irrigation (Objective 1, H1) 50
5.2 Irrigation Water Productivity (Objective 2, H2) 50
5.3 Soil Hydraulic Function—K_{fs} (Objective 3, H3) 51
5.4 VWC Dynamics (Objective 3, continued) 53
5.5 Hydraulic-Yield Relationships (Objectives 4 and 5, H5) 54
5.6 Practical Implications for Southwest Kansas 55
5.7 Limitations 56
5.8 Recommendations for Future Research 57
5.9 Conclusions 58
References 60
APPENDICES 70
APPENDIX A - Statistical Analysis Methods and Complete ANOVA Tables 71
A.1 Experimental Design: Split-Plot RCBD 71
A.2 F-Statistic Notation and Interpretation 72
A.3 Standard Errors and Confidence Intervals 73
A.4 ANOVA Assumptions 73
A.4.1 Normality of Residuals 73
A.4.2 Homogeneity of Variance 74
A.4.3 Independence of Observations 74
A.4.4 Balance 74
A.5 Spearman Rank Correlation 75
A.6 Complete Split-Plot ANOVA Tables — All Response Variables 75
A.7 Statistical Decision Map 79
APPENDIX B - Split-Plot ANOVA PYTHON Code 80

APPENDIX C - IBI Biochar Certification Document 84
APPENDIX D - SERVITECH Soil Labratory Report 85

List of Figures

Figure 1.1 Conceptual yield-water production function and irrigation water productivity 4
Figure 2.1 Water-level changes in the High Plains (Ogallala) Aquifer from predevelopment to 2017..... 3
Figure 2.2 conceptual framework diagram 18
Figure 3.1 Location of the Southwest Research-Extension Center (SWREC) study site in Finney County, Garden City, Kansas, USA..... 22
Figure 3.2 SATUO infiltrometer field photograph 29
Figure 4.1 Daily precipitation (mm) and reference evapotranspiration (ET alfalfa and ET grass, mm d^{-1}) during the 2025 corn growing season (June 11–November 6, Garden City, Kansas). 35
Figure 4.2 Corn grain yield (Mg ha^{-1}) as a function of irrigation treatment, SWREC Garden City, Kansas, 2025. 38
Figure 4.3 Effect of application rate of biochar and APSA-80 on corn grain yield (Mg ha^{-1}) using (a) W100 and (b) W50 irrigation methods at SWREC, Garden City, KS, 2025..... 39
Figure 4.4 (a) Individual plot K_{fs} ($\times 10^{-3}$ cm s^{-1}) from pre-treatment to post-treatment, with colored lines indicating irrigation regime assignment. Large symbols show irrigation regime means ± 95% CI; small lines show individual subplots. (b) K_{fs} fold-change (post/baseline) by APSA-80 × irrigation treatment, with individual subplot observations. 43
Figure 4.5. Volumetric water content (VWC, %) measured 24 h after irrigation (solid lines) and at the pre-irrigation trough (dashed lines) by corn growth stage and irrigation treatment. .. 46
Figure 4.6. Between-event soil water drawdown (pp = post-irrigation VWC minus trough VWC) by corn growth stage and irrigation treatment. 46
Figure 4.7. Volumetric water content (VWC, %) at corn harvest (November 6–7, 2025) by irrigation treatment..... 47
Figure 4.8. Spearman rank scatter plots: (a) pre-irrigation trough VWC (%) vs. yield ($\rho = +0.377$, $p = 0.024$, *); (b) between-event drawdown (pp) vs. yield ($\rho = -0.314$, $p = 0.062$, †); (c) post-treatment Kfs (cm s^{-1}) vs. yield ($\rho = +0.048$, NS). 49

List of Tables

Table 2.1. Summary of key studies by measurement scope, showing the gap filled by this study. ✓ = measured; — = not measured; * = this study. 19

Table 3.1. Pre-treatment baseline soil physical and chemical properties by experimental block, 0–15 cm depth, SWREC Garden City, Kansas, July 2025 (ServiTech Laboratories, Lab Nos. 122479–122484). 21

Table 3.2. Treatment factors, irrigation levels, application rates, and application dates—2025 corn experiment, SWREC, 2025 23

Table 3.4. Physicochemical properties of the IBI-certified granular softwood biochar applied in this study, as determined by IBI-accredited laboratory analysis. 24

Table 3.5. Crop season timeline and key management events, SWREC Garden City, Kansas, 2025 27

Table 3.6. Seasonal water budget by irrigation treatment, SWREC Garden City, Kansas, 2025. 28

Table 4.1. Monthly rainfall, reference evapotranspiration (grass reference crop and alfalfa reference crop), and number of irrigation applications for the 2025 corn growth season at SWREC Garden City. 34

Table 4.2. Corn grain yields descriptive statistics by irrigation regime, SWREC Garden City, Kansas, 2025. 37

Table 4.3. Split-plot ANOVA for corn grain yield, SWREC Garden City, Kansas, 2025. 37

Table 4.4. Descriptive corn grain yield means (bu ac^{-1}) and standard deviations for all irrigation × biochar × APSA-80 treatment combinations, SWREC Garden City, Kansas, 2025. n = 3 per combination. 38

Table 4.5. Split-plot ANOVA for irrigation water productivity (IWP, kg ha^{-1} mm^{-1}), SWREC Garden City, Kansas, 2025. 40

Table 4.6. Pre-treatment and post-treatment K_{fs} summary and ANOVA for K_{fs} fold-change, SWREC Garden City, Kansas, 2025. 41

Table 4.7. ANOVA for K_{fs} fold-change (post-treatment K_{fs} / baseline K_{fs}), SWREC Garden City, Kansas, 2025. 42

Table 4.8. K_{fs} fold-change means by Irrigation × APSA-80 combination, SWREC, 2025. n = 9 per combination; 95% CI from subplot residual (df = 20; $t_{0.025,20}$ = 2.074). 42
Table 4.9. VWC response means irrigation F-tests (whole-plot error, df = 2), SWREC, 2025. VWC measured at 10 cm depth. Dir. = directional pattern; no formal F-test at individual stage level (see note). 44
Table 4.10. Between-event VWC drawdown (pp) at 10 cm depth by growth stage and irrigation treatment, SWREC, 2025. n = 18 per treatment × stage. 45
Table 4.11. Spearman rank correlations (ρ) between plot-level hydraulic indicators and corn grain yield (n = 36 plots), SWREC Garden City, Kansas, 2025. NS = not significant; † p < 0.10; * p < 0.05. 48
Table A.1. Degrees of freedom partitioning for the split-plot RCBD, SWREC, 2025. 72
Table A.2. F-statistic notation guide with critical values and examples. 72
Table A.3. Standard error formulas and 95% CI half-widths for treatment means (grain yield example). 73
Table A.4. Shapiro-Wilk test for normality of ANOVA model residuals, SWREC, 2025. 74
Table A.5. Spearman rank correlations between hydraulic indicators and grain yield (n = 36 plots), SWREC, 2025. VWC at 10 cm depth. 75
Table A.6. Split-plot ANOVA for grain yield (bu ac^{-1}). MS_WP = 214.36 (df=2); MS_SP = 136.25 (df=20). 76
Table A.7. Split-plot ANOVA for irrigation water productivity (IWP; kg ha^{-1} mm^{-1}). MS_WP = 2387.2 (df=2); MS_SP = 3.934 (df=20). 76
Table A.8. Split-plot ANOVA for Kfs fold-change. MS_WP = 0.01247 (df=2); MS_SP = 0.01247 (df=20). 77
Table A.9. Split-plot ANOVA for pre-irrigation trough VWC (10 cm depth, %). MS_WP = 6.847 (df=2); MS_SP = 1.242 (df=20). 77
Table A.10. Split-plot ANOVA for between-event VWC drawdown (10 cm depth, pp). MS_WP = 12.563 (df=2); MS_SP = 3.666 (df=20). 78
Table A.11. Split-plot ANOVA for VWC at harvest (10 cm depth, %). MS_WP = 19.408 (df=2); MS_SP = 2.124 (df=20). 78
Table A.12. Statistical decision map—justification for each analytical choice. 79

Acknowledgements

Completion of the master's thesis is a result of the hard work of several people, who provided advice, assistance, and encouragement on my way to this result. I would like to express gratitude to all of them.

First, I would like to thank my major professor, Dr. Jonathan Aguilar, for his mentorship, high intellectual level, and patience during this project preparation from its very beginning till its completion. It was a great pleasure for me to work under your supervision. You challenged my views, increased my knowledge in soil and irrigation science, and gave me a chance to create something valuable. I feel extremely lucky to have had such a wonderful mentor.

I would also like to thank my co-major advisor and members of the graduate advisory committee, Dr. Vaishali Sharda and Dr. Ganga Hettiarachchi, for your constructive feedback and valuable input. I would also like to thank Dr. Araya Berhe for their mentorship and support throughout my graduate studies.

This research was conducted at the Southwest Research Extension Center (SWREC) in Garden City, Kansas. I am extremely thankful to Dr. Farzam Moghbel, Dr. Okubay Adhanom, and WSREC staff for their logistical support during the 2025 growing season. I would also like to thank my graduate colleagues from the Department of Biological and Agricultural Engineering at Kansas State University. I would also like to thank the MICRA (Microbial Innovation for Climate-Resilient Agriculture) project and its team.

Finally, I am extremely thankful to my family for unconditional love and unwavering support throughout my graduate studies. Your encouragements and patience during this journey have meant more than words can express.

Dedication

This thesis is dedicated to the farming communities of the High Plains whose livelihoods rely on an invaluable commodity. The Ogallala Aquifer has been feeding the world for years now. Let's hope the science we create today will make sure it keeps doing just that in the future.

Chapter 1 - Introduction

1.1 Background and Problem Statement

The Ogallala (High Plains) Aquifer spans roughly 450,000 km² across eight states, stretching from South Dakota to Texas, and provides the primary water source for irrigated agriculture in the western part of the Great Plains (McGuire & Strauch, 2022). The Ogallala Aquifer in Kansas covers the western one-third of the state. It provides water to irrigate more than 2.7 million acres, producing agricultural products important not only to Kansas but also to the entire country (Steiner et al., 2021; Whittemore et al., 2023). However, the intensive extraction of groundwater over many years, which has been taking place at a rate much higher than the natural recharge of 0.6–2.5 cm per year, has led to a water level decline of 30–60 meters in southwest Kansas compared to the pre-development period (McGuire & Strauch, 2022; Whittemore et al., 2023). The depletion trend hasn't reversed to date, even when accounting for data up to 2019 (McGuire & Strauch, 2024).

Haacker et al. (2016) found that water depletion is expected in major parts of Kansas and Texas over the coming decades due to water extraction, which could jeopardize irrigated corn production in these areas. Steward and Allen (2016) calculated water depletion in the High Plains Aquifer from 1930 to 2110. They predicted that maximum depletion rates would continue into mid-century under business-as-usual scenarios, with no opportunity for recovery on a human timescale. As aquifer levels decline, less water will be available for well yields and higher pumping lifts, making it doubtful whether complete evapotranspiration replacement irrigation is economically sustainable for growers in Finney, Haskell, and Grant counties (Steiner et al., 2021). Growers can already quantify the economic implications of this depletion scenario at the farm level. The greater the decrease in the aquifer's saturated thickness, the greater the increase in pumping cost, the lower

the well yield, and thus the higher the cost of pumping one acre-foot of water. Therefore, this scenario reduces profit margins for irrigated corn farms that rely on competitive access to water. Araya et al. (2019) quantified the economic value of water producing major irrigated crops in the Ogallala Aquifer region. The researchers found that although irrigated corn provides the highest economic benefit per unit of water among the major crops in the Ogallala Aquifer region, this advantage depends highly on the amount of water applied per acre. Higher pumping costs and potential water allocation limits under the strategic goal of Kansas Groundwater Management District No. 3 make the economic benefits of deficit irrigation, which produces potential production with smaller water use, increasingly evident (Araya et al., 2019; Steiner et al., 2021).

Aquifer depletion in this region is compounded by climate change dynamics. Warmer temperatures in the southern Great Plains in recent decades have led to higher seasonal reference evapotranspiration rates, and future warming scenarios indicate even warmer years ahead, creating greater discrepancies between crop water demand and supply (IPCC, 2021; Kukal & Irmak, 2018). Araya et al. (2017) suggest that maize yields on irrigated farmland in Kansas will decline under high-emission warming scenarios without adaptive measures, making water-saving methods even more crucial. Under conditions of decreasing supply and increasing demand, improving water-use efficiency to obtain as much product per millimeter of groundwater applied has become a necessity for local agriculture. The method of deficit irrigation, which involves providing water amounts below the amount necessary to completely replace crop evapotranspiration (ET_c), has been the most widely studied (English, 1990; Rudnick et al., 2019; Aguilar et al., 2023).

1.2 Deficit Irrigation as a Water Conservation Strategy

Deficit irrigation allows controlled plant water stress when crop yield responsiveness is low. It reduces yield while saving much more water than is lost due to the yield reduction. From an agricultural viewpoint, the basis for deficit irrigation is the non-linear dependence of yield on the volume of irrigated water: the marginal increase in yield per liter of water diminishes as irrigation approaches full replacement of ET_c.

An extensive literature review on deficit irrigation practices in the High Plains Aquifer system by Rudnick et al. (2019) found that deficit irrigation at a 50% ET_c level using various irrigation practices usually results in a 10 to 18% loss in corn yields but a 40 to 55% reduction in groundwater abstraction and thus overall improved irrigation water productivity (IWP). Araya et al. (2021) also evaluated optimal irrigation strategies for maize grown in western Kansas. They concluded that moderate deficit practices yield positive water productivity under limited well capacity, as in Ogallala operations. The field trial conducted at SWREC in Garden City, Kansas, by Aguilar et al. (2023) demonstrated the applicability of deficit irrigation considering the specific well-capacity limitations of southwest Kansas. Stepanovic et al. (2021) also demonstrated the important role of maize hybrids in regulating water productivity under deficit irrigation conditions in semi-arid Nebraska. Igwe et al. (2025) demonstrated that properly designed deficit irrigation practices enable the attainment of adequate yields while significantly reducing groundwater depletion under extreme climatic conditions.

However, the size of the yield versus water trade-off ratio is flexible, depending on the water storage capacity of the soil, timing of precipitation, hybrid water tolerance, and the hydraulic characteristics of the soil in terms of infiltration, retention, and delivery of water to plants. For this

reason, this research simultaneously assesses soil hydrological functioning and its influence on yield and IWP.

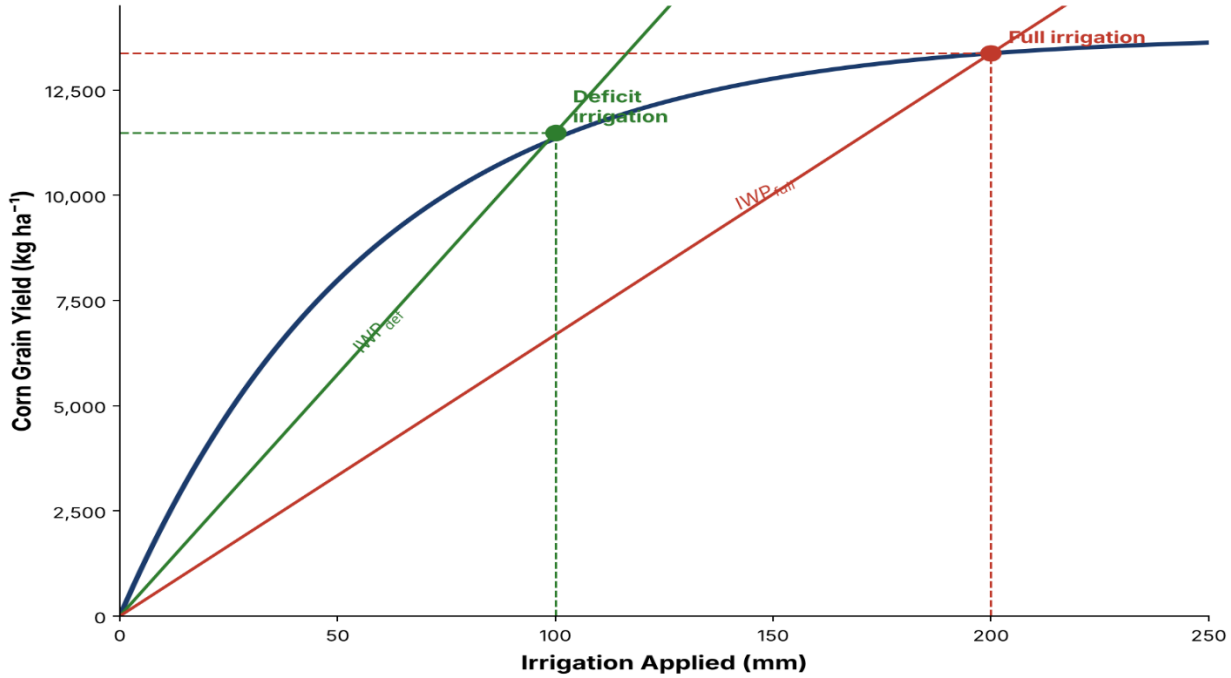


Figure 1.1 Conceptual yield-water production function and irrigation water productivity

1.3 Soil Hydraulic Function and Its Role in Irrigation Performance

The role of soil hydraulic properties, including infiltration, redistribution, retention, and drainage, is fundamental to determining how effectively applied water is converted into crop-available soil moisture. The field-saturated hydraulic conductivity (K_{fs}) is an indicator of how rapidly water can infiltrate the soil when applied under near-saturated field conditions and is especially significant in the case of sprinkler irrigation in which water must first infiltrate at the soil surface before entering the root zone (Reynolds & Elrick, 2002; Ritchie, 1981). If K_{fs} are impaired by the development of a surface seal from irrigation cycles of wetting and drying, the infiltration rate will decrease, leading to surface ponding and runoff (Levy & Mamedov, 2002). Changes in volumetric

water content (VWC) indicate the soil's ability to store and release water between irrigations. They can be used to estimate the amount of root-zone water available between irrigation applications (Ritchie, 1981).

Although these hydraulic functions are recognized as critical to understanding the yield effects of deficit irrigation, only a handful of field experiments in the High Plains have characterized K_{fs} and VWC dynamics alongside yield and IWP. Thus, knowledge of the hydraulic mechanisms governing the effects of irrigation management on crop response under local soil and production conditions in southwest Kansas remains limited.

1.4 Soil Amendments: Biochar and APSA-80

The two soil amendments utilized in this experiment for the purpose of improving soil hydraulic efficiency in conditions of reduced irrigation include (1) certified granular softwood biochar, which meets the IBI (International Biochar Initiative) standards, and (2) a non-ionic soil surfactant called APSA-80. Biochar is a recalcitrant form of pyrogenic carbon produced by the pyrolysis of organic materials under limited oxygen conditions. This material has received significant scientific attention due to biochar's ability to influence soil hydraulic properties (such as soil water retention, soil hydraulic conductivity, and soil pore structure) (Blanco-Canqui, 2017; Razzaghi et al., 2020; Edeh et al., 2020; Lehmann et al., 2021). It has been established by Weber & Quicker (2018) that feedstock and pyrolysis temperature determine the physical and chemical properties of biochar for its use in soil hydraulics. Various meta-analyses show that biochar has significant positive impacts on crop yield and water-use efficiency in cropping systems worldwide and that these impacts increase over time as it integrates into the soil matrix (Han et al., 2023; Jiang et al., 2024; Acharya et al., 2024). It should be noted that, in addition to being an agricultural amendment, biochar has

also proven to be a climatic change mitigation strategy, as it is a stable pyrogenic carbon that persists in soils for decades to centuries. In this experiment, biochar has been applied using subsurface inter-row banding at a depth of 10 centimeters (about 3.94 in). It should be noted that this approach differs from the surface broadcasting of biochar, which is predominant in the published literature, due to the material's low bulk density (0.066 g cm^{-3}) (Graves, 2013; Gabhane et al., 2020).

1.5 Study Motivation and Significance

The current research is inspired by the convergence of practical needs and scientific opportunities associated with corn irrigation in southwest Kansas. From a producer's perspective, increased depletion of the Ogallala and possible water allocation limitations set by Groundwater Management District No. 3 can make deficit irrigation inevitable (Steiner et al., 2021; Whittemore et al., 2023). Economic water productivity analysis made by Araya et al. (2019) showed that irrigated corn yields the greatest economic gains per unit of water used in the Ogallala; improving IWP is a direct means of increasing farm resilience to water allocation restrictions. The information needed by producers is not whether deficit irrigation decreases yield (it will), but rather how much, under which soil conditions, and whether some soil hydraulic management practices can diminish the yield loss.

From a scientific perspective, the concurrent analysis of soil hydraulic properties, yield, and IWP in a split-plot deficit-irrigation × soil-amendment experiment provides a mechanistic basis for understanding the response to water stress that is currently missing from the High Plains agronomy literature. Two soil amendments investigated in the current study, biochar and APSA-80, represent different approaches to soil hydraulic properties manipulation: the former is an immediate

modification of the soil structure and capacity due to physical and chemical integration into the soil matrix for several seasons (Acharya et al., 2024; Jiang et al., 2024), while the latter operates at the water-soil interaction stage to provide immediate improvements of irrigation event uniformity (Feng et al., 2002; Kostka, 2000). The assessment of these amendments' effectiveness under different irrigation conditions, along with the characterization of soil hydraulic properties at pre- and post-treatment stages, enables the creation of a multi-season evaluation framework to track the development of hydraulic amendment effects. The 2026 follow-on experiment at SWREC, including the Bacillus biosurfactant inoculation test conducted with two different soil types, expands the hydraulic baseline established in this study.

1.6 Research Objectives

The objectives of this first-season field study were to:

1. Examine the impact of W100 and W50 deficit irrigations on the grain yield of corn at the SWREC, Garden City, Kansas, in the year 2025.

2. Measure water productivity and total water productivity with respect to W100 and W50 irrigations and evaluate the agricultural justification for adopting deficit irrigation due to constraints on water allocation from the Ogallala aquifer.

3. Study the dynamics of K_{fs} and VWC under different irrigation regimes and the effect of biochar and APSA-80 amendments on these variables.

4. Explore the extent to which soil hydraulic function variables (fold change in K_{fs}, between-event VWC reduction, and pre-irrigation trough VWC) provide a mechanistic basis for plot-scale variability in corn grain yield.

5. Examine whether the first-year application of biochar (0, 1, and 3.5 t ha^{-1}) and APSA-80 causes changes in soil hydraulic properties in the anticipated direction.

1.7 Research Hypotheses

H1. A 50% reduction in irrigation water applied will significantly reduce corn grain yield compared to complete irrigation, but the growing-season precipitation pattern will mitigate the effect.

H2. Irrigation deficits will lead to significantly higher IWP than at complete irrigation levels, since the reduction in water applied exceeds the reduction in grain yield.

H3. Application of APSA-80 will change the value of K_{fs} and the dynamics of VWC between events, resulting in less surface hydraulic disturbance and more uniform water redistribution, depending on the amount of irrigation applied in each event.

H4. In the first growing season, biochar applications will have no significant impact on corn grain yield and IWP, since biochar effects in fine-textured soils require multiple seasons of soil integration to manifest.

H5. The values of plot-level soil hydraulic variables, such as the pre-irrigation trough VWC and VWC between events, may predict variations in corn grain yield.

This is a sound scientific choice, since biochar's impact on soil hydraulic properties is time-dependent and increases over several growing seasons. The impacts become increasingly pronounced as the soil is amended over several seasons, as evidenced by research findings

(Blanco-Canqui, 2017; Lehmann et al., 2021). Year one established a baseline for amendment effects but do not reflect their long-term effect.

1.8 Thesis Organization

Chapter 2 provides a detailed review of the literature divided into nine sections on the Ogallala Aquifer and sustainability of irrigation in southwest Kansas; climate change as one of the compounding factors in increasing irrigation demands; concepts of deficit irrigation, approaches, and yield trade-offs; water productivity indicators in irrigated corn cultivation; soil hydraulic functions and their measurements; biochar characteristics, hydraulic impact, crop yields, and biochar application approaches; APSA-80 surfactant characteristics and soil hydraulic redistribution, including new bio-surfactant alternative APSA-80; and research gaps that this study fills. Chapter 3 gives the study location description, research design, treatments, data collection methodology for K_{fs}, VWC, grain yields, IWP, and climate data, and statistical analysis procedures. Chapter 4 presents results based on research objectives. Chapter 5 analyzes results in relation to hypothesis and literature, evaluates the practical and economic implications of irrigated corn cultivation in Southwest Kansas, recognizes the limitations of this study, and formulates conclusions and recommendations for further research, including the planned experiment for 2026. Appendix A gives complete ANOVA tables and statistical assumptions. Appendix B presents a statistical analysis code. Appendices C and D include the biochar certification report of IBI and the soil laboratory test report of ServiTech, respectively.

Chapter 2-Literature Review

The literature review of this chapter will discuss the scientific background for each of the five research objectives stated in the introduction chapter, going from the regional scale of groundwater sustainability in southwest Kansas up to the scale of agronomic practice of deficit irrigation, metrics of water productivity, soil hydraulic function, and the impact of biochar and APSA-80 amendment on physical and hydraulic properties of soils.

2.1 Semi-Arid Irrigated Agriculture in Southwest Kansas

Southwest Kansas is one of the regions with the highest degree of agricultural irrigation in the U.S., including cultivation of corn (Zea mays L.), grain sorghum (Sorghum bicolor L. Moench), winter wheat (Triticum aestivum L.), and alfalfa (Medicago sativa L.) in Finney, Haskell, and Grant counties and nearby Seward and Stevens counties using irrigation with groundwater. The climate of the region is semi-arid continental with an annual mean precipitation of 460 mm in Garden City, high radiation of the sun, low relative humidity, constant southerly winds causing high evaporation, and variable yearly precipitation, which makes unirrigated corn cultivation unreliable (Patrignani et al., 2020; Araya et al., 2021).

Corn cultivation in the southern High Plains has grown significantly in recent decades due to high yields and demand for corn from nearby ethanol production facilities and animal farms. Seasonal water needs of the corn crop are about 550-700 mm, so it is one of the most intensively irrigated crops in the region. Considering the semi-arid climate in Finney County, additional irrigation of 150-250 mm or more is needed to cover the seasonal water demands of corn crops in almost all years (Stone et al., 2008; Rudnick et al., 2019). The center pivot irrigation system is the most widely used overhead sprinkler system in the High Plains area, as it is efficient and works well

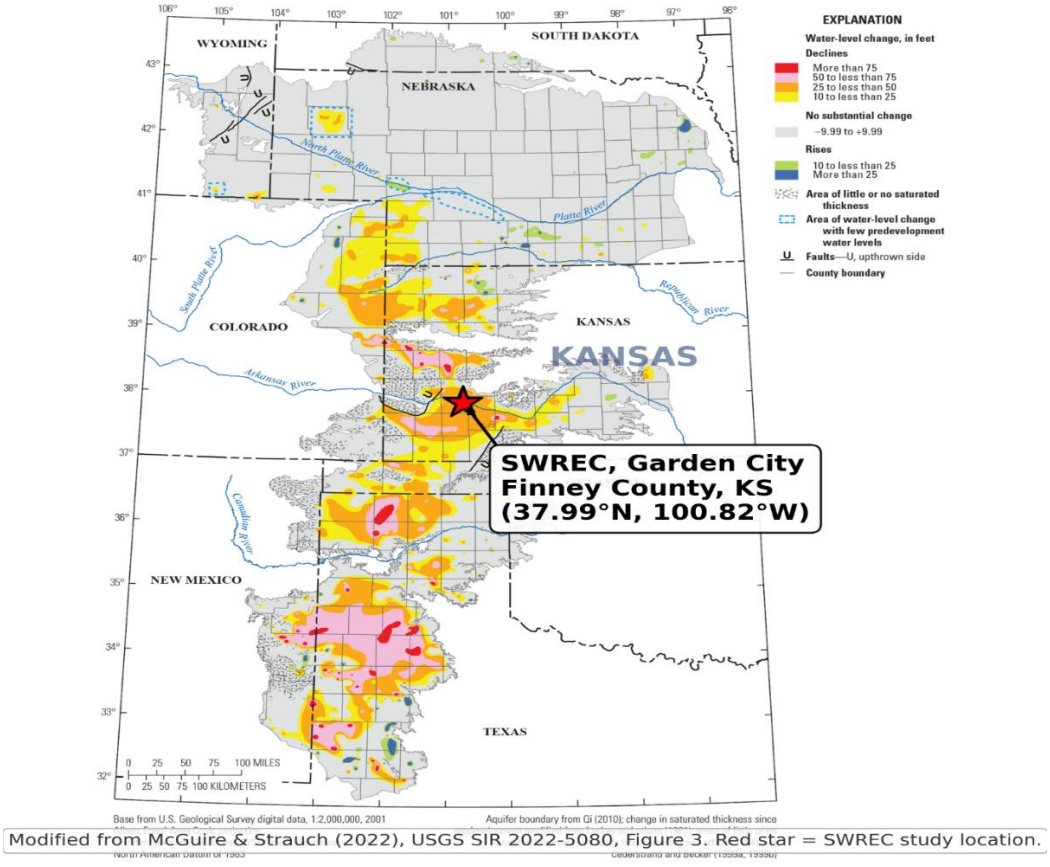
with square and circular fields (Rudnick et al., 2019). The linear move irrigation system uses a lateral pipe equipped with overhead sprinklers that moves in a straight line through a rectangular field. This irrigation system is employed in the area, as the field shape and high discharge capacity of wells make it appropriate. Steiner et al. (2021) discussed various policies, techniques, and methods of saving Ogallala water in Kansas. Deficit irrigation was identified as one of the most applicable ways to reduce pumping rates.

2.2 High Plains Aquifer Depletion and Irrigation Sustainability

The High Plains Aquifer is a regional aquifer system that consists mainly of Ogallala Formation sediments that were formed during the Miocene and Pliocene eras by alluvial fans transporting sediments from the Rocky Mountains to the east with little sediments from other geological formations (McGuire & Strauch, 2022). The Ogallala Formation constitutes the primary saturated formation of the High Plains Aquifer and serves as the primary source of water for irrigating agriculture in southwest Kansas. The natural replenishment of the aquifer system is extremely small (between 0.6 and 2.5 cm yr^{-1}) because of the presence of impermeable sedimentary rock layers over the aquifer system (McGuire & Strauch, 2022).

Groundwater extraction for irrigation purposes started in the 1950s, gained momentum in the 1970s, and continued in the 1980s, causing an imbalance between extraction and recharge and leading to an irreversible drop of the groundwater table. According to McGuire and Strauch (2022), mean water levels declined by 4.0 meters during 1950-2017 in the High Plains Aquifer, and declines exceeded 30 meters in some regions of southwest Kansas. Information on water levels updated through 2019 shows that this trend was not reversed (McGuire & Strauch, 2024). The latest data on the status of the High Plains Aquifer in Kansas in 2023 show that the mean saturated

thickness of the Kansas Ogallala part of the aquifer has decreased by 15.2 meters from predevelopment until 2023, and the mean water levels have decreased by 0.9 meters over the last two years (Whittemore et al., 2023). Haacker et al. (2016) found in their research that, according to current extraction trends, serious economic problems caused by aquifer depletion will emerge across large parts of Kansas and Texas within several decades. Steward and Allen (2016) found that, for the year 2110, peak depletion will continue into the mid-century with almost no recharge.



Modified from McGuire & Strauch (2022), USGS SIR 2022-5080, Figure 3. Red star = SWREC study location.

Figure 2.1 Water-level changes in the High Plains (Ogallala) Aquifer from predevelopment to 2017.

2.2.1 Climate Change as a Compounding Driver of Irrigation Demand

In turn, climate change adds to the pressure from aquifer depletion, causing both higher seasonal evaporative demand and greater precipitation unpredictability during growing seasons. Observed

warming in the Great Plains over recent decades has contributed to higher seasonal reference evapotranspiration (IPCC, 2021). Kukal and Irmak (2018) found that climate variability affects crop yields in the U.S. The Great Plains have become increasingly important in recent decades, with rising temperatures increasing instability in irrigated corn yields. Anandhi (2016) found that changes in the accumulation of growing degree days in Kansas contribute to earlier corn phenological development, thereby shortening the VT–R2 reproductive period. Araya et al. (2017) predicted a meaningful decrease in irrigated corn yields in Kansas under the high emission scenario without any adaptive measures. Similarly, Li and Troy (2018) noted that climate change reduced the response of irrigated crop yields in the western U.S., highlighting the need for water-saving adaptations in the region.

In a recent study on the adaptive approach to deficit irrigation management under extreme climatic conditions, with the help of the DSSAT-CERES corn model used in Finney County, Kansas, it was shown by Igwe et al. (2025) that the use of deficit irrigation based on ET can reduce losses in the yield of maize by approximately 10 percent while saving 25 percent of water during conditions of extremely hot and dry weather.

2.3 Deficit Irrigation: Definitions, Approaches, and Trade-offs with Yields

Deficit irrigation may be considered an approach that involves partial replacement of ET_c, allowing the plant to sustain a controlled deficit when yield is highly sensitive to water stress (English, 1990). Economic justification of deficit irrigation is based on the concavity of the production function between crop yield and irrigation levels because the marginal increase in crop yield for the marginal increment in irrigation level is lower for irrigation levels approaching the replacement

of ET_c, thus ensuring that IWP = grain yield/irrigation is maximized (English, 1990; Molden et al., 2010).

Corn is somewhat drought-tolerant, but the tasseling stage through the early silking stage (VT–R2) is the most vulnerable to water stress, during which pollination may cause kernel abortion, leading to excessive yield losses given the deficit volume (NeSmith & Ritchie, 1992). At the same time, Rudnick et al. (2019) demonstrated in the High Plains Aquifer that deficit irrigation (50% ET_c) decreases corn yields by 10 to 18% while saving 40 to 55% of water, thereby increasing IWP. Thus, according to Klocke et al. (2011), yield loss for a 50% deficit in multi-year field trials in western Kansas was 15%. Stone et al. (2008) found that the yield–water curve is asymmetric and that yield losses are lower than water savings for moderate-deficit volumes across different High Plains locations. Aguilar et al. (2023) investigated new deficit irrigation approaches, including partial root zone deficit (PRD) and regulated deficit irrigation (RDI). The research was conducted in corn production in western Kansas at SWREC, showing high yields when using PRD compared to normal irrigation. Araya et al. (2021) also reported that moderate deficit irrigation produced favorable results for water productivity in western Kansas. Also, Stepanovic et al. (2021) have noted the impact of hybrid choice on water productivity in semiarid Nebraska under deficit irrigation.

2.4 Water Productivity Metrics in Irrigated Corn Production

2.4.1 Irrigation Water Productivity vs. Total Water Productivity

Productivity of water in irrigated agriculture can be measured using two metrics, namely irrigation water productivity (IWP = yield/irrigation applied) and total water productivity (TWP = yield/(irrigation + precipitation)). From an economic decision-making perspective, the IWP metric

should be used because it directly accounts for the profitability of each unit of groundwater utilized (English, 1990; Molden et al., 2010).

The two measurements can be applied to different management questions. The IWP is the better measurement of the two when it comes to assessing water use efficiency in the Ogallala region since it measures the amount of profit obtained from each unit of pumped groundwater, the constraining factor under Kansas allocation rules (English, 1990; Molden et al., 2010; Araya et al., 2019). The TWP includes irrigation and precipitation and is the better metric to apply when one is looking at the whole system water use efficiency, regional hydrology, or policies that involve the total water input (Zwart & Bastiaanssen, 2004; Molden et al., 2010). The two measurements are included in this paper because they are answering different questions related to water efficiency.

2.4.2 Typical IWP Values for Irrigated Corn in the High Plains

A review of a study of crop water productivity for irrigated wheat, rice, cotton, and maize, based on 25 global experiments by Zwart and Bastiaanssen (2004), reported irrigated corn CWP values between 0.77 and 1.68 kg m^{-3} (equivalent to 7.7–16.8 kg ha^{-1} mm^{-1}). In the High Plains region, the IWP values for full irrigation are between 40 and 80 kg ha^{-1} mm^{-1} depending on the hybrid, soil type, and seasonal rainfall, while deficit irrigation has been proven to raise IWP values to 80-130 kg ha^{-1} mm^{-1} (Rudnick et al., 2019; Stepanovic et al., 2021). In addition, Li et al. (2016) found that in semi-arid irrigated agricultural systems, irrigation management practices were the main contributors to IWP variability, compared with climate-related factors.

2.5 Soil Hydraulic Function and Irrigation Performance

2.5.1 Field-Saturated Hydraulic Conductivity (K_{fs})

Field saturated hydraulic conductivity (K_{fs}) describes the rate at which water travels through the soil when the soil is near saturation in the field, and this property accounts for macroporosity, aggregate stability, and pore connectivity (Reynolds & Elrick, 2002). K_{fs} is a key parameter in assessing the efficiency of an irrigation system that applies water through overhead irrigation, such as linear move or center pivot sprinkler irrigation. In such a case, the water needs to travel from the soil surface to the plant roots. If K_{fs} is reduced due to a surface seal, water could enter the soil surface more slowly than it is applied (Levy & Mamedov, 2002).

In agricultural soils, the value of K_{fs} is affected by past management practices; irrigation leads to the movement of fine particles, soil dispersion, and pore sealing, which gradually reduce K_{fs} as surface seals develop (Levy & Mamedov, 2002). Seasonal reduction in K_{fs} due to irrigation practices is a well-known problem that reduces irrigation efficiency, thus presenting a hydraulic basis for the effects of amendments studied in this experiment. The SATURO dual-head automatic tension infiltrometer used in this experiment calculates the value of K_{fs} based on the steady-state infiltration rate measured under two positive heads using the Wooding (1968) dual-head solution, without the need for separate determination of the α^* capillarity parameter, unlike the single-head method (Reynolds & Elrick, 2002).

2.5.2 Volumetric Water Content Dynamics and Irrigation Interpretation

Continuous data from volumetric water content (VWC) sensors deployed in situ reflect the soil water cycle, characterized by rapid water recharge after each irrigation, followed by redistribution and drainage, and a gradual reduction in soil water content between events due to crop transpiration

and soil evaporation. The difference between the maximum values reached immediately after the end of each irrigation and the minimum value before the next irrigation is a composite of all processes occurring between events and reflects a whole-system soil-water depletion rate (ΔVWC; Ritchie, 1981). In the case of deficit irrigation, decreased water applications per irrigation event mean that less water reaches the root zone, while water demand continues, leading to faster soil water depletion. Báťková et al. (2023) confirmed that the properties of soils' hydraulic functions, such as K_{fs}, correlate strongly with soil water retention and storage capacity.

2.6 Biochar: Properties, Hydraulic Effects, and Amendment Considerations

2.6.1 Biochar Characterization and Soil Carbon Sequestration

Biochar is a highly porous carbon material created through the heating of organic matter between temperatures of 300 and 800 degrees Celsius in a limited supply of oxygen (pyrolysis), thus creating a stable carbon-rich material that can have a high surface area, high microporosity, and a long soil life of decades to millennia (Lehmann et al., 2021). A thorough review of the physical and chemical properties of biochar by Weber and Quicker (2018) reveals that both the feedstock type and pyrolysis temperature are the major factors determining biochar properties significant for agricultural soil applications. The specific surface area, porosity distribution, bulk density, and surface chemistry also play significant roles. Wang and Wang (2019) conducted a literature review on biochar production and its environmental applications. They stated that the high specific surface area and microporosity of pyrogenic carbon from lignocellulosic feedstock were among the main mechanisms of biochar's action on soil water properties and carbon sequestration (Lehmann et al., 2021).

2.6.2 Biochar Effects on Soil Hydraulic Properties

The results of meta-analysis have shown that biochar addition promotes higher water retention in soil, but the effect largely depends on the soil's texture. Razzaghi et al. (2020) conducted a systematic review and meta-analysis of 82 scientific studies. They reported that biochar had a significant positive effect on soil water content at field capacity across all soil textures, with the greatest effect on coarse soils and a decreasing effect on fine soils. Edeh et al. (2020), based on a meta-analysis of 37 scientific studies, found that biochar increased available water content by 28.5% and field capacity by 20.4%. Novak et al. (2012) demonstrated significant improvements in water-holding capacity in Ultisol and two types of Aridisols after laboratory incubation with softwood-derived biochar. Wang et al. (2019) conducted a multi-scale study and found that biochar improves water retention in various agricultural soils by enhancing macropores and intra-aggregate water-holding capacity.

Several factors, including context-dependence and texture specificity, influence the impact of biochar on K_{fs}. For example, Gelardi et al. (2021) showed that biochar affected the hydraulic conductivity of two types of agricultural soils, with the effect depending on the application rate, soil texture, and biochar feedstock. Hassan et al. (2022) investigated the impacts of biochar on K_{fs} in a sandy loam soil, the same type as the Ulysses silt loam in the current study. They reported that the application rate and biochar particle properties were the main factors affecting the response during the first season. The opposite findings were obtained by Castellini et al. (2014) in clay soil, where biochar decreased hydraulic conductivity by altering the pore structure. Blanco-Canqui (2017) conducted a thorough review of the literature on biochar impacts under field conditions and suggested that the effects of biochar in fine-textured soils at rates below 5 t ha^{-1} are relatively small during the first season of application. This finding is a scientific basis for Hypothesis H4.

However, the time-dependent nature of the effects of biochar amendments is a crucial aspect of biochar assessment that is frequently overlooked. In their recent review of biochar effects on soil water dynamics, Acharya et al. (2024) reported that the impact of biochar amendments on soil water dynamics in fine-textured soils does not occur within the first year of application and usually increases over two to five years due to weathering, fragmentation, and physical integration of biochar particles into soil aggregates, resulting in an increasing surface area of interaction between biochar and soil matrix and in changes in the interaggregate pore size. Aller et al. (2018), in a field experiment investigating the long-term impact of biochar applications on corn yield, soil quality, and economic viability in the U.S. Midwest, found that the effects of biochar amendments on soil water retention and soil physical properties accumulate from year to year. The maximum positive effects on soil properties appeared by the end of the third year after the application of amendments. Similar results have been reported by Kang et al. (2022), who conducted a literature review of biochar soil amendment studies and found that water retention effects increased over time, with the highest in fine-textured soils. All these studies demonstrate the need for the present study's chosen approach, based on 2025 data: it is necessary to establish the trajectory of hydraulic effects rather than the terminal state of soil-water dynamics.

2.6.3 Biochar and Crop Yield

A large body of literature is available on the effect of biochar application on crop yield across various cropping systems and climates, all of which indicate a positive average effect, with significant heterogeneity among studies. For instance, in the seminal meta-analysis of biochar applications in agriculture, Jeffrey et al. (2015) found an average yield increase of ~10% across all cropping systems but extremely high heterogeneity, since biochar effects on yields were strongly dependent on biochar characteristics, soil characteristics (soil pH and soil texture), and

climatic factors. It turned out that the biochar effect on yields was significantly greater in acidic and infertile soils than in buffered agricultural soils, indicating that yield effects in irrigation systems for high-yield corn production (southwest Kansas) have a hydraulic nature and are not connected to soil fertility.

Other meta-analyses also addressed the topic. For instance, in the meta-analysis of 142 publications by Han et al. (2023), the authors demonstrated that biochar application led to an 11.2% increase in yield, a 12.3% increase in water use efficiency, and an 8.7% increase in nitrogen use efficiency. This combination of agronomic benefits is particularly relevant to deficit irrigation in Southwest Kansas. Another meta-analysis by Jiang et al. (2024) on the global long-term impact of biochar on yield showed that yield effects strengthen as the number of years since application increases, with the best results achieved after three or more years. This meta-analysis directly supports the multi-year evaluation protocol needed to evaluate the biochar effect in the current study. Yield effects at the sub-5-t-ha^{-1} biochar rates used in this study (1 and 3.5 t ha^{-1}), in fine-textured agricultural soils, are rare in the first season, as was shown by Blanco-Canqui (2017) and Edeh et al. (2020).

In semi-arid irrigated cropping environments, where water limitation, rather than fertility, becomes a limiting factor for crop yield, the agronomic pathway to yield improvement is increased soil water retention and reduced water stress accumulation between events (Acharya et al., 2024; Razzaghi et al., 2020). This hydraulic pathway is precisely why the simultaneous characterization of K_{fs} and VWC is needed in the current study. This hydraulic data allows for an understanding of the reasons behind yielding responses to biochar and their occurrence in particular years.

2.6.4 Biochar Application Methods, Wind Displacement, and Cost Considerations

The application method is a key design criterion for biochar addition, strongly influencing the magnitude of hydraulic changes and the economic feasibility of implementation. Most of the studies in the literature feature surface broadcast followed by tillage incorporation, a combination appreciated for its simplicity and compatibility with standard farm machinery (Graves, 2013; Gabhane et al., 2020). Surface broadcasting allows even distribution of biochar across the field, and, as a result, it's evenly mixed with the topsoil during tillage incorporation. However, in the no-tillage approach used in SWREC, biochar applied via broadcasting cannot be incorporated using tillage practices. Therefore, when biochar is broadcasted in no-till, it will mostly stay on or close to the soil surface, where it will be more vulnerable to displacement by wind because of the very low bulk density (0.066 g cm^{-3}) of the material and its lowest impact on the root zone water transport characteristics (Graves, 2013). To solve these issues, the current experiment utilized inter-row banding at 10-cm depth instead of surface broadcasting.

Aerosol movement is among the most significant practical constraints in surface broadcasting biochar applications, particularly granular or fine particle biochar, which is mostly produced from wood-based materials. The IBI-certified granular softwood biochar used in the current study has a density of about 0.066 g cm^{-3}; hence, it is much less dense than the loam soil in southwest Kansas by more than 20 times. This means that the biochar material is highly susceptible to being moved by winds during surface broadcasting under such conditions in southwest Kansas. As reported by Graves (2013), aerosol transportation before and after surface broadcasting is associated with substantial losses of the biochar material when the bulk density is less than 0.1 g cm^{-3}. In the current study, the use of 10-cm depth inter-row bands was selected to avoid this problem. Subsurface inter-row band placement, which was implemented in the current study and involved

placing the material at a depth of 10 cm between corn rows, excludes this risk of aerosol transport and ensures even and accurate delivery of the specified rate to the target zone, increasing the efficiency of the treatment in comparison with surface broadcast (Gabhane et al., 2020).

The economic feasibility of the treatment is another crucial, often overlooked criterion that determines its viability. Many studies, in which a significant impact of biochar on soil and crop yield was proven, used rates of 5 to 20 t ha^{-1} or higher, which would make such treatments economically impractical at current commercial prices of USD 500 to 3,000 per ton of biochar, depending on the feedstock and certification, thus totaling in USD 2,500 to 60,000 per hectare (Aller et al., 2018; Jeffery et al., 2015). Rates of 1 and 3.5 t ha^{-1} considered in the current study are specifically chosen as producer-feasible ones, that is, they fall within the economically reasonable range of application. Subsurface band placement enables the achievement of the desired volumetric concentration in the inter-row root zone at lower application rates.

2.7 APSA-80: Surfactant Properties and Soil Hydraulic Redistribution

In general, soil surfactants are substances that decrease the contact angle between water and soil particles, thereby improving soil water distribution and reducing soil water repellency (Kostka, 2000). APSA-80 (All-Purpose Spray Adjuvant) is a non-ionic surfactant characterized by Mukherjee et al. (2009) as having a critical micelle concentration of about 0.006 g%, reducing water surface tension from 72 mN m^{-1} (pure water) to about 20 mN m^{-1}. Therefore, under an overhead linear-move irrigation regime, when irrigation water is applied in direct contact with the soil surface, APSA-80 is expected to improve infiltration uniformity and reduce preferential flow paths, thereby forming a localized surface seal. In a field study of the effects of the application of non-ionic surfactant to loamy agricultural soils under overhead irrigation, Almaz et al. (2023)

reported significant effects on the hydraulic conductivity of the soil and water distribution, with irrigation intensity being a factor that modifies the effect of surfactant application, as it was found in this study in relation to a significant irrigation × APSA-80 interaction on K_{fs}. According to Kostka (2000), the use of surfactants in turfgrass management greatly decreased the water-repellent properties of soils by altering soil hydraulic function, as investigated in studies of corn cultivated under field conditions.

The mechanism by which non-ionic surfactants such as APSA-80 affect soil's ability to infiltrate water operates at the interface between water and soil particle surfaces. In soils showing partial or incipient water repellence, an effect that occurs when there is partial water repellence of the soil by accumulating hydrophobic coatings of organic compounds on the mineral surfaces due to extensive irrigation, the contact angle between the advancing water and the surface of the particle is above 90°, preventing water from penetrating fine pores and forcing the water to pass through larger conductive channels (Feng et al., 2002). The reduction of the contact angle below the critical value by adsorption at the interface and a decrease in the surface tension of the applied water enable the non-ionic surfactant to restore conditions for water wetting and increase water distribution (Feng et al., 2002; Kostka, 2000). It was shown in a controlled experiment by Feng et al. (2002) that the application of a non-ionic surfactant to water-repellent soil significantly increases the cumulative infiltration rate and improves the uniformity of wetting-front penetration compared to water without surfactant addition, depending on the level of water repellency. In overhead linear-move irrigation systems, where the applied water directly contacts the soil surface, adding surfactants may help prevent unfavorable infiltration conditions by mitigating the progressive development of surface water repellency.

2.7.1 Biological Surfactants: Bacillus-Derived Surfactin as a Natural Analog to Synthetic Soil Surfactants

In addition to synthetic surfactants like APSA-80, a promising class of soil-wetting agents is provided by biological surfactants secreted by soil microorganisms. One of the strongest biosurfactants currently known is surfactin, a cyclic lipopeptide biosurfactant secreted by Bacillus subtilis and related Bacillus species. This biosurfactant exhibits extremely high activity, reducing water surface tension to about 27 mN m^{-1} when added to soil solution at a concentration as low as 0.005%, comparable to that of artificial surfactants, including APSA-80 (Gutierrez et al., 2022; Abdoli et al., 2025). The ability of Bacillus-containing soil to generate surfactin in situ without additional artificial amendments seems promising for the sustainable management of soil water content and the reduction of soil hydraulic repellency in irrigated agricultural systems.

In their paper, Gutierrez et al. (2022) assessed the effects of Bacillus subtilis inoculation and purified surfactin on the dynamics of evaporation from soils of loam and sandy loam texture, which are the soil texture types relevant to the soil of this study, as well as to the two experimental fields of the 2026 follow-up experiment. These authors have found that both Bacillus subtilis inoculation and surfactin application significantly reduce the rate of water evaporation from the tested soils compared with the uninoculated control, while loam soils exhibit a greater absolute improvement in water retention than sandy loam soils at equal biosurfactant concentrations. The texture dependence of the biosurfactant effect on soil hydrology properties was explained in the work of Gutierrez et al. (2025) by the modulation of soil water retention and wetting capacity through changes in the surface area, pore size distribution, and the ability of soil particles to adsorb biosurfactant, which provides a rationale for the use of soils with different textures in the 2026 follow-up experiment at SWREC.

From the practical viewpoint, the use of biosurfactants in agriculture was summarized in the review of Abdoli et al. (2025), where Bacillus-derived surfactin has been discussed as one of the promising biosurfactants for enhancing soil water retention and wettability in semi-arid agricultural areas due to the possibility of creating a sustainable soil microbial population that will provide continuous soil improvement. In his doctoral dissertation at Kansas State University, Gutierrez (2025) demonstrated that Bacillus subtilis and surfactin amendments enhance water retention in agricultural soils under semi-arid High Plains conditions, providing an experimental foundation for the 2026 Bacillus inoculation treatments at SWREC. The findings presented above motivate the inclusion of Bacillus inoculation as a treatment in the 2026 follow-up experiment.

2.8 Relationships Between Soil Hydraulic Function and Crop Outcomes Under Deficit Irrigation

The relationship between soil hydraulic behavior and crop yield in a deficit irrigation system using overhead linear move irrigation systems is straightforward. Under overhead irrigation, water should infiltrate through the soil surface, travel through the soil profile, and be retained in the root zone. As the value of K_{fs} decreases due to the formation of a surface seal, as reported in the present study, the infiltration rate at the soil surface slows, which may result in ponding, uneven distribution, or runoff at high application rates. Levy and Mamedov (2002) suggest that repeated irrigation can lead to a gradual decrease in K_{fs} due to the formation of a surface seal throughout the season.

Enhanced water-holding capacity of the soils and reduced depletion of VWC between events ensure higher soil moisture content before irrigation, thereby decreasing the accumulation of the water stress deficit and affecting the physiological processes that determine crop yield, especially

during the VT-R2 reproductive stage (NeSmith & Ritchie, 1992). Thus, in the linear move irrigation system, both K_{fs}, responsible for surface water infiltration, and VWC dynamics, responsible for root zone water availability between events, are agronomic indicators. The research by Li et al. (2016) demonstrated that management practices affect soil hydraulic parameters, which are the main determinants of IWP variation in semi-arid irrigated agricultural systems.

2.9 Research Gaps Addressed by This Study

- Gap 1. Few studies in scientific literature have conducted field measurements of K_{fs} and VWC along with grain yield and IWP in a deficit irrigation experiment using the linear move-overhead irrigation method under High Plains conditions to characterize the hydraulic processes influencing yield response.
- Gap 2. The scientific literature lacks field-scale characterization of the impacts of granular softwood biochar (dominant particle diameter of 4-8 mm) on K_{fs} and VWC in loamy-textured soils under semi-arid conditions with linear move irrigation.
- Gap 3. Despite the broad use of APSA-80 in turf management, few scientific publications examine its application in irrigated annual grain crops under an overhead irrigation system in a semi-arid region.
- Gap 4. No single field experiment examined the effects of deficit irrigation, biochar, and APSA-80 on soil hydraulic properties and crop performance under High Plains conditions.

2.10 Conceptual Framework and Literature Summary

Figure 2.2 shows the conceptual model linking irrigation regime and soil amendment inputs to soil hydraulic behavior and agricultural outcomes. In linear-move overhead irrigation, the surface infiltration capacity of K_{fs} determines whether the irrigation water infiltrates into the root zone,

ponds, or runs off. In addition, the dynamics of VWC show how efficiently water is retained for subsequent crop use. Both soil hydraulics indicators have agronomic meaning in this case. Precipitation is another water source, influenced by irrigation and soil hydraulics, and it determines the total water input to the plant. The presented research incorporates all elements of the framework into a single first-season field trial.

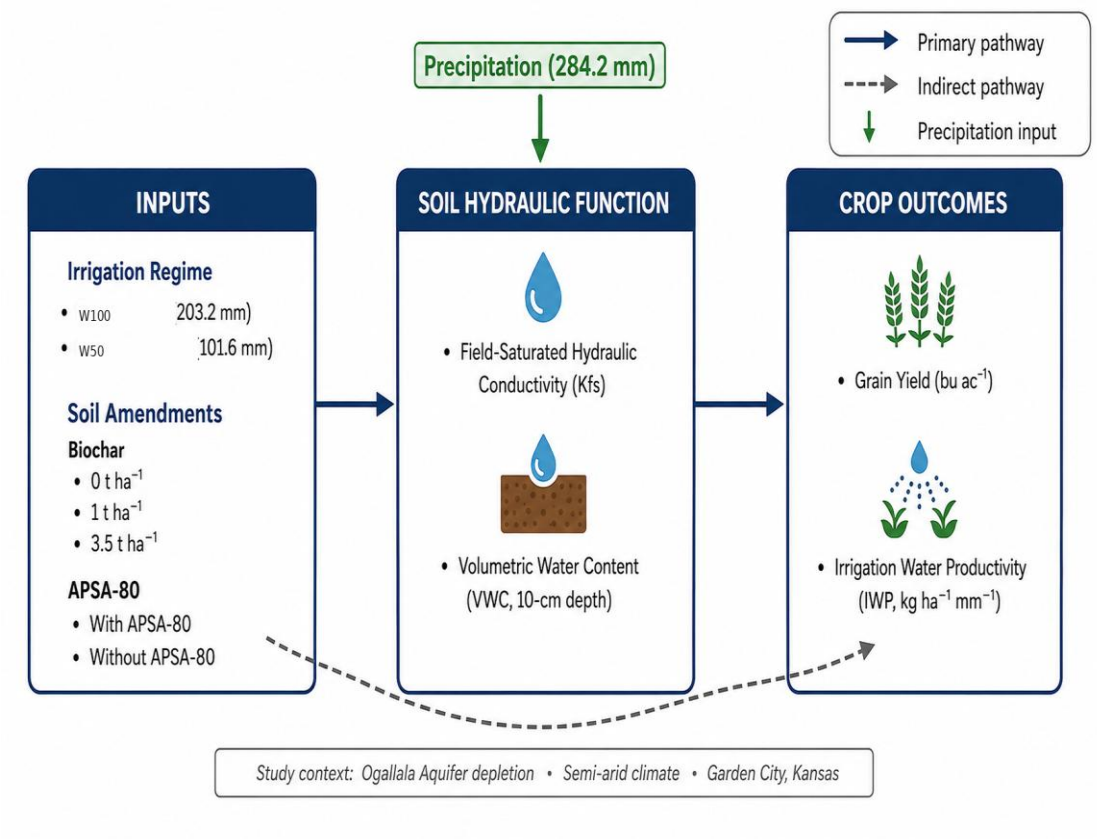


Figure 2.2 conceptual framework diagram

Table 2.1. Summary of key studies by measurement scope, showing the gap filled by this study. ✓ = measured; — = not measured; * = this study.

Study	Location/Soil	Treatment	Yield	IWP	K_{fs}	VWC	Amendment
Klocke et al. (2011)	W. Kansas, loam	Full vs. deficit ET_c	✓	✓	—	—	None
Stone et al. (2008)	High Plains, varied	Full vs. deficit	✓	✓	—	—	None
Rudnick et al. (2019)	High Plains review	50% ET_c deficit	✓	✓	—	—	None
Araya et al. (2021)	W. Kansas maize	Optimal irrigation	✓	✓	—	—	None
Stepanovic et al. (2021)	W. Nebraska, sandy	Deficit + hybrids	✓	✓	—	—	None
Razzaghi et al. (2020)	Meta-analysis (82)	N/A	—	—	—	✓	Biochar
Edeh et al. (2020)	Meta-analysis (37)	N/A	—	—	✓	✓	Biochar
Novak et al. (2012)	Ultisol/Aridisols	N/A	—	—	—	✓	Biochar
Gelardi et al. (2021)	Two ag. soils	N/A	—	—	✓	—	Biochar
Almaz et al. (2023)	Loamy soil, irrigated	Nonionic surfactant	—	—	✓	✓	Surfactant
This study*	SWREC, silt loam	Full vs. 50% deficit	✓	✓	✓	✓	Biochar + APSA

Chapter 3 - Materials and Methods

3.1 Study Site and Soil Characterization

The experiment was performed in the experimental field of the Southwest Research-Extension Center (SWREC) of Kansas State University, Garden City, Finney County, Kansas (37.9897° N, 100.8151° W; elevation 879 m above sea level; Figure 3.1). SWREC is the major KSU research site for irrigated crop production research in the semi-arid southern High Plains. It has been actively involved in research on water management and soil amendments for over five decades (Patrignani et al., 2020).

The climate of the region is classified as semi-arid continental with an average annual rainfall of about 460 mm in Garden City, intense solar radiation, low relative humidity, prevalence of southerly winds, thus creating high evaporation demands, and interannual rainfall variability, making rain-fed corn production unsustainable long-term (Patrignani et al., 2020; Araya et al., 2021). Evaporation-transpiration (ET) losses during the growing season are significantly higher than rainfall, necessitating additional groundwater irrigation to sustain corn farming in the region. The long-term average reference ET (ET alfalfa) for the growing season in Garden City is 962 mm, while only 349 mm of precipitation on average falls approximately 600 mm short of ET demand (Araya et al., 2017). The groundwater aquifer that serves as the region's water source is the High Plains (Ogallala) Aquifer. It is characterized by a significant decline in water levels due to over-exploitation that exceeds replenishment rates, especially over the last decades (McGuire & Strauch, 2022; Whittemore et al., 2023).

The soil type in the experimental field is Ulysses silt loam (fine-silty, mixed, super-active, mesic Aridic Haplustolls), a deep, highly permeable soil order of Mollisol developed from loess deposits

typical of most upland agricultural soils of southwest Kansas. The characteristic features of such a soil type are the relatively even texture of the soil surface layer, a higher moisture storage capacity than sandy soils, and the possibility of forming surface seals under high irrigation intensity (Levy & Mamedov, 2002).

Baseline soil samples before treatment application were taken from composite soil subsamples (0-15 cm depth) in June 2025 and analyzed by ServiTech Laboratories in Dodge City, Kansas (Lab Nos. 122479 to 122484). The summary of soil properties is given in Table 3.1 for each replicate block. The average soil properties of the surface layer were pH 7.1, OM 1.93%, and CEC 20 meq 100 g^{-1}, and the particle size distribution was 30.6% sand, 44.2% silt, and 25.3% clay, which corresponds to the loam to clay loam on the surface, as well as the fine-silty soil family classification of the Ulysses silt loam soil type. The field had previously been cultivated with corn under no-till conditions.

Table 3.1. Pre-treatment baseline soil physical and chemical properties by experimental block, 0–15 cm depth,

Property	Block 1 (T1–T6)	Block 1 (T7–T12)	Block 2 (T1–T6)	Block 2 (T7–T12)	Block 3 (T1–T6)	Block 3 (T7–T12)	Mean
pH (1:1 water)	7.0	6.3	7.4	6.8	7.0	7.0	7.1
Organic matter (%)	1.7	2.1	2.2	1.7	1.8	2.1	1.9
CEC ($cmol_+ kg^{-1}$)	19	17	23	17	21	23	20
Sand (%)	30.7	31.2	28.3	31.6	32.7	28.8	30.6
Silt (%)	45.0	45.5	44.5	43.5	42.4	44.2	44.2
Clay (%)	24.3	23.3	27.2	24.9	24.9	27.0	25.3
Texture class	Loam	Loam	Clay loam	Loam	Loam	Clay loam	Loam
EC (mmho cm^{-1})	1.10	0.73	1.29	0.85	0.99	0.98	0.99
Nitrate-N (mg kg^{-1})	47.4	58.2	64.2	60.1	69.1	68.1	61.2

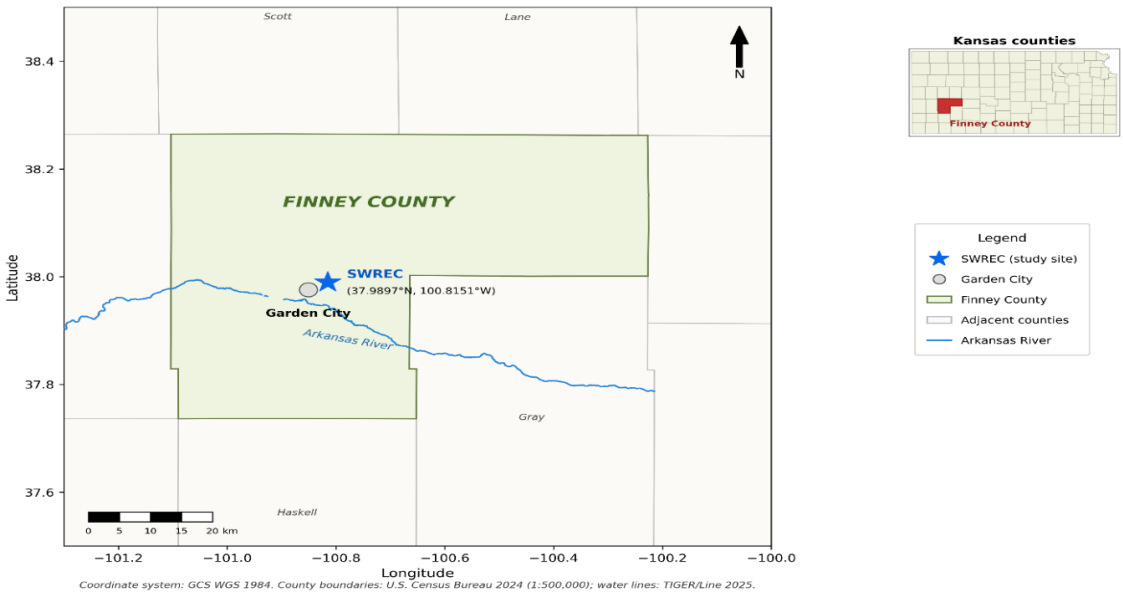


Figure 3.1 Location of the Southwest Research-Extension Center (SWREC) study site in Finney County, Garden City, Kansas, USA.

3.2 Experimental Design

The experiment was arranged as a balanced split-plot randomized complete block design (split-plot RCBD) with three replicate blocks. The reason why this particular design was used for the study is that, while irrigation is applied on a large scale as in the entire field (as the main plot) by the linear move system, the soil amendment treatment is applied at the subplot scale, hence requiring the split-plot error partitioning described in the following paragraphs (Gomez & Gomez, 1984; Montgomery, 2017). The whole-plot factor was chosen as irrigation to contrast different soil moisture environments, in which the effects of the subplot factors would be compared, in line with the scientific aim of studying the effects of full and deficit irrigation on biochar and APSA-80 performance.

Irrigation was the whole-plot factor with two levels of full irrigation (Full; 203.2 mm seasonal total) and 50% deficit irrigation (Deficit; 101.6 mm). The six subplot treatment combinations were

randomized in each main plot (block × irrigation) as follows: Three biochar rates (0, 1, and 3.5 t ha^{-1}) crossed with two APSA-80 levels (with and without), giving 3 × 2 = 6 subplot combinations in each main plot. Total number of subplots = 3 blocks × 2 irrigation levels × 6 subplot combinations = 36. Table 3.2 lists the factors and their levels.

Table 3.2. Treatment factors, irrigation levels, application rates, and application dates

Factor	Level	Description	Rate / Amount	Application date
Irrigation (Main Plot)	W100	Maximum well-capacity irrigation	203.2 mm	8 events, Jun 18 – Aug 23
	W50	50% full volume per event	101.6 mm (4.0 in) seasonal	8 events, Jun 18 – Aug 23
Biochar (Subplot)	B0	Unamended control	0 t ha^{-1}	—
	B1	IBI-certified granular	1 t ha^{-1} (dry wt. basis)	June 21
	B3.5	IBI-certified granular	3.5 t ha^{-1} (dry wt. basis)	June 21
APSA-80 (Subplot)	S0	No surfactant (control)	—	—
	S1	APSA-80	30 oz ac^{-1} per application	emergence (~Jun

3.3 Corn Production and Agronomic Management

A Pioneer brand corn hybrid, P0487Q, was planted on June 11, 2025, at a seeding rate of 75,000 plants ha^{-1} (30,360 plants ac^{-1}) using row spacing of 0.76 m (30 inches) in a no-till system. The emergence of the corn plants was recorded on June 18, 2025. All agronomic management techniques, such as fertilization, weed control, and pest management, were performed consistently in all plots.

Corn grain was harvested manually on November 6-7, 2025, during which ears of corn from two rows in the middle of the plot were collected. The total length of the rows in this case was 3.05 m

(10 ft). The area of the plot where harvesting took place is 4.65 m². After that, ears of corn were shelled using a David Bradley Electric Corn Sheller. The mass of grain harvested was measured using a Mettler Toledo SB32001DR scale. Moisture content of the grain was analyzed using a Dickey-John GAC II grain moisture meter. The yield was adjusted to 15.5% moisture content and expressed in bu/ac with conversions into kg/ha when necessary (1 bu/ac corn = 62.77 kg/ha).

3.4 Biochar Amendment Characteristics and Application

This study used IBI-certified granular softwood biochar. Ten days after corn sowing, biochar was added to the soil in the designated subplots in the subsurface and inter-row layers at a depth of 10-15 cm to minimize wind erosion and provide biochar close to the crop roots. Biochar was added in amounts of 0 (control), 1, and 3.5 t ha^{-1} (dry mass basis). Properties of the used softwood biochar, as determined by an IBI-accredited laboratory, are shown in Table 3.4.

Table 3.4. Physicochemical properties of the IBI-certified granular softwood biochar applied in this study, as determined by IBI-accredited laboratory analysis.

Property	Value	Unit	Analytical method
Feedstock	Softwood	—	—
Bulk density	0.066 (4.1 lb cu ft^{-1})	g cm^{-3}	ASTM D1762-84
Organic carbon (OC)	85.7	% dry mass	ASTM D4373
pH	8.21	units	USCC Rajkovich
Electrical conductivity	0.142	dS m^{-1}	USCC Rajkovich
H:C molar ratio	0.47 (IBI max = 0.70)	molar ratio	IBI certification
Specific surface area	232	m^2 g^{-1}	Butane correlation
Total nitrogen	0.89	% dry mass	Dry combustion
Dominant particle size	4–8 mm (45.5% by mass)	mm	ASTM D2862
Volatile matter	24.5	% dry mass	ASTM D1762-84
Heavy metals	Below are IBI limits.	mg kg^{-1}	EPA 3050B/6020

Biochar was incorporated using subsurface inter-row placement at a depth of about 10 cm between the corn rows of each biochar-treated plot. This method was chosen because (1) the amendment would be concentrated in the root zone area; (2) it would ensure local relevant volumetric concentration of the amendment at the feasible nominal rates of the producer; (3) it would avoid upward migration due to buoyancy of the low-density granular biochar (bulk density 0.066 g cm^{-3}, 20 times lighter compared to the surrounding loamy soil) under saturated irrigation conditions; and (4) it would not conflict with no-till farming. The 4–8 mm granular particle size creates discrete macropores in the inter-row soil zone upon incorporation, altering local soil pore structure (Lim et al., 2017; Blanco-Canqui, 2017).

Biochar application rates of 0, 1, and 3.5 t ha^{-1} were recorded as based on the entire field area, following the convention in the agronomic literature. As the biochar was applied only in a subsurface inter-row band (with 30 cm width, 10 cm depth in between the corn rows), the local concentration in the treated band was more intense than indicated by the field application rate. The broadcast equivalent rate was determined as follows:

Broadcast-Equivalent Rate (t ha^{-1}) = Field Rate (t ha^{-1}) × [Row Spacing (cm) ÷ Band Width (cm)]

= Field Rate × (76.2 cm ÷ 30 cm) = Field Rate × 2.54

For the 30 cm wide band, which covered 39.4% of the inter-row (as the row spacing was 76.2 cm), the broadcast-equivalent rates for 1 and 3.5 t ha^{-1} field rates were 2.54 and 8.89 t ha^{-1}, and the corresponding concentrations in the bands were 0.20 and 0.68% w/w, respectively. The calculated broadcast equivalent rates were within the ranges of those known to show progressive effects in hydraulic and yield response in fine-textured agricultural soils in consecutive seasons (Acharya et al., 2024; Kang et al., 2022; Jiang et al., 2024).

3.5 APSA-80 Application

The All-Purpose Spray Adjuvant, which is a nonionic surfactant (APSA-80), was sprayed twice using a dosage of 30 oz ac^{-1}, firstly soon after emergence and then as a side dress on July 10, 2025, about two weeks after biochar application as a surface spray to the subplots during the early vegetative stage of growth (V4-V5). The spraying was carried out with the understanding that it would be incorporated through irrigation and would be effective at the soil surface during irrigation, since active surface sealing occurs during this period (Kostka, 2000; Mukherjee et al., 2009; Almaz et al., 2023).

3.6 Irrigation Management and Scheduling

The irrigation method used in the experiment was a linear move sprinkler system, which uses a lateral pipe supported on wheels and equipped with overhead sprinklers that move along the field in a straight line, irrigating an area equal to the field width. Water was applied to the field surface with overhead sprinklers and then infiltrated downward through the Ulysses silt loam to the root zone. The well capacity is insufficient to irrigate at levels of full ET replacement. All W100 irrigated plots received 1.0 in (25.4 mm) per event, based on the practical application of the well capacity used in SWREC. In contrast, W50 plots received exactly 0.5 (12.7 mm), resulting in a 50% volume reduction at each irrigation application. Such a proportional arrangement of irrigation events ensures that both W100 and W50 irrigation have the same frequency, thus making the total applied water volume the only manipulated variable (English, 1990; Rudnick et al., 2019).

Irrigation events were scheduled using soil moisture monitoring information and Kansas Mesonet reference evapotranspiration data through the KanSched3 scheduling tool (Patrignani et al., 2020). Irrigation was done eight times between June 18 and August 23, 2025. The last irrigation event

was applied on August 23 based on the SWREC staff's assessment of crop water requirements, well allocation availability, and the crop's nearing physiological maturity. Total seasonal irrigation amounts were 203.2 mm (8.0 in) and 101.6 mm (4.0 in) for W100 and W50 irrigations, respectively. The complete timeline of the crop season is summarized in Table 3.5, and the seasonal water budget for each irrigation treatment is presented in Table 3.6.

Table 3.5. Crop season timeline and key management events, SWREC Garden City, Kansas, 2025.

Event	Date	Details
Corn planting	June 11	Pioneer P0487Q; 75,000 plants ha^{-1}; 0.76-m rows; no-till
Crop emergence	June 18	7 days after planting;
Pre-treatment K_{fs}	Before June 17	3 SATURO infiltrometer; inter-row position
Biochar application	June 21	Subsurface inter-row band; 10 cm depth; 0, 1, 3.5 t ha^{-1}
Irrigation event 1	June 18	W100 = 25.4 mm; W50 = 12.7 mm; linear move
APSA-80 application	June 18	Surface spray; 30 oz ac^{-1}; soon after emergence
	July 10	30 oz ac^{-1}; V4–V5 growth stage
Irrigation events 2–7	July 11–Aug 15	W100 = 25.4 mm each event; W50= 12.7 mm each event
Irrigation event 8 (last)	August 23	W100= 25.4 mm; Deficit = 12.7 mm
Post-treatment K_{fs}	October 1–5, 2025	36 measurements; same subplot locations as pre-treatment
Corn harvest	November 6–7	Hand harvest: 2 center rows × 10 ft per subplot
Grain shelling	December 17	David Bradley electric corn sheller

Table 3.6. Seasonal water budget by irrigation treatment, SWREC Garden City, Kansas, 2025.

Water source	W100 irrigation (mm)	W50 irrigation (mm)
Applied irrigation (8 events)	203.2	101.6
Irrigation-period precipitation (Jun 11–Aug 23)	92.5	92.5
Post-irrigation precipitation (Aug 24–Nov 6)	191.8	191.8
— of which September	115.1	115.1
Total growing season precipitation (Jun 11–Nov 6)	284.2	284.2
Total seasonal water input	487.4	385.8
Difference (W100 – W50)	101.6 mm (20.8%)	—
Approx. % of seasonal corn ET_c (~625 mm)	~77.9%	~61.7%

3.7 Field-Saturated Hydraulic Conductivity (K_{fs}) Measurement

Field saturated hydraulic conductivity (K_{fs}) was determined using the METER SATURO dual-head single-ring automatic tension infiltrometer (METER Group, Inc., Pullman, WA) according to the manufacturer's specifications. SATURO employs two sequential positive-pressure heads in a single soil ring inserted 10 cm deep at the inter-row location, producing infiltration data recorded over time. From these data, K_{fs} is calculated using the dual-head analytical solution of Wooding (1968) with paired steady-state infiltration rates. In the dual-head technique, the α^* capillarity parameter need not be estimated independently, as in the single-head case, thereby greatly minimizing uncertainty in K_{fs} estimation in a field environment with heterogeneous spatial distributions of hydraulic properties (Reynolds & Elrick, 2002). Measurement of K_{fs} at 10 cm ring insertion depth is suitable for determining the surface soil hydraulic properties responsible for infiltration of irrigated water in this linear move irrigation system, since infiltration starts at the soil surface and depends on the hydraulic properties of the near-surface soil horizon.

Field saturated hydraulic conductivity measurement took place once for each subplot: (1) pre-treatment, that is, before biochar and APSA-80 were applied to the soil, and (2) post-treatment, that is, before the completion of the growing season. The rings were inserted to a depth of 10 cm at the same position as the biochar, and measurements were taken for 120 minutes until a steady state was reached. Pre-treatment and post-treatment K_{fs} measurements were recorded for the same position in the subplot by the same operator. K_{fs} fold-change was calculated as the ratio of post-treatment to pre-treatment K_{fs} per subplot (fold-change = K_{fs}_post / K_{fs}_pre).



Figure 3.2 SATURO infiltrometer field photograph

3.8 Volumetric Water Content (VWC) Monitoring

The volumetric water content (VWC) of the soil was continuously recorded by Acclima TDR sensors placed approximately 10 cm (4 in) deep in the center of each subplot between corn rows 2 and 3. Each subplot had one Acclima TDR sensor (n = 36). The sensors were pre-calibrated in the factory for mineral soil and linked to a central data logger via independent cables. The installation

depth of 10 cm was chosen since this would allow us to measure soil water dynamics in the upper layer of the soil that is most affected by irrigation, evaporation, and root water uptake.

The VWC measurements were recorded at discrete points in time for each of the eight irrigations: 24 hours after each irrigation (post-irrigation VWC) and within 2 hours before the next irrigation (pre-irrigation through VWC). The pairing of the measurements facilitates the determination of the between-event VWC change (ΔVWC = post-irrigation VWC – trough VWC, percent point), reflecting the between-event soil water removal caused by crop transpiration, soil evaporation, and drainage. Four corn growth stages were monitored: V6-V7, V8-V9, V10-V11, and VT. Pre-treatment VWC was recorded, as was VWC at harvest time (November 6-7, 2025).

3.9 Irrigation Water Productivity (IWP) and Total Water Productivity (TWP)

The Irrigation Water Productivity (IWP; kg ha^{-1} mm^{-1}) was computed for each treatment plot by dividing the moisture-corrected grain yield (kg ha^{-1}) by total seasonal irrigation (mm) according to the methods of English (1990) and Zwart and Bastiaanssen (2004). The Total Water Productivity (TWP; kg ha^{-1} mm^{-1}) was computed by dividing the yield (kg ha^{-1}) by the sum of the seasonal irrigation and seasonal precipitation (mm). These two indices are provided because they address different questions about groundwater management (IWP) and total water use efficiency (TWP). Seasonal irrigation of 203.2 mm (W100) and 101.6 mm (W50) was used for all IWP computations.

3.10 Climate and Evapotranspiration Data

Meteorological data measured daily, including precipitation, temperature, solar radiation, wind speed, and relative humidity, were provided by the Kansas Mesonet automated weather station located at Garden City/SWREC (Kansas Mesonet, 2025), which is an accurate monitoring system throughout the state according to Patrignani et al. (2020). The daily reference evapotranspiration

(evapotranspiration from grass and alfalfa) was collected from the automated weather station for Garden City/SWREC from the Kansas Mesonet website (Kansas Mesonet, 2025) and uses the standardized FAO-56 Penman-Monteith equation for calculating the daily ET (Allen et al., 1998). Dates of data collection span from June 11 to November 6, 2025.

3.11 Statistical Analysis

All dependent variables were analyzed using a balanced split-plot design with an appropriate sum-of-squares decomposition for the split-plot RCBD experiment (Gomez & Gomez, 1984; Montgomery, 2017). Decomposition of the total SS included: SS_Total = SS_Blocks + SS_Irrigation + SS_Block×Irrigation + SS_Biochar + SS_APSA + SS_Biochar×APSA + SS_Irrigation×Biochar + SS_Irrigation×APSA + SS_Irrigation×Biochar×APSA + SS_SubplotResidual. The effect of irrigation was compared with the mean square (MS) of Block × Irrigation, the whole-plot error source, with 1 df in the numerator and 2 in the denominator. All subplot factors were tested for their effects using the subplot residual MS (df = 20).

Statistical significance was declared at $\alpha = 0.05$. Results that showed a p-value of $0.05 \leq p < 0.10$ have been indicated by marginal trend (†) and considered in relation to the low power of the whole plot design at df = 2 (F critical = 18.51 at $\alpha = 0.05$). EMMs with standard errors (SE) have been calculated using appropriate MS error values. For the irrigation main effect, the 95% confidence interval was calculated using the critical t-value with df = 2 ($t_{0.025,2} = 4.303$).

Spearman rank correlations (ρ) between plot-level soil hydraulic variables and grain yield (n=36 plots) were calculated as an initial exploration of hydraulic-yield relationships. The use of Spearman rank correlation in place of Pearson is warranted here due to (1) the nonlinearity of the relationships between hydraulic parameters and yield; (2) the often right-skewed nature of K_{fs} with

potentially influential outliers for which Spearman rank correlation is more robust; and (3) the sample size n=36 does not provide sufficient power to identify moderate correlations, thus Spearman rank correlation is more adequate for identifying directional trends. In view of the simultaneous testing of several hydraulic parameters, the interpretation of the results is treated as directional evidence supporting mechanistic hypotheses. The $\log_{10}$ transformation of K_{fs} variables was applied before ANOVA to achieve normality of the residuals. Means were back transformed to the original measurement scale. VWC data from four growth stages per plot were pooled into a single plot-level average before ANOVA to prevent pseudo-replication of correlated repeated measures within each plot (Girden, 1992). All statistical analyses were performed in Python 3.11 using a custom split-plot ANOVA function written from first principles, with F-distribution probabilities computed using SciPy. Stats and Spearman correlations computed using SciPy.stats. spearmanr (NumPy 1.24; pandas 2.0; SciPy 1.11).

Chapter 4 - Results

In this chapter, the results of the 2025 corn production growing season experiment at the Southwest Research-Extension Center (SWREC), Garden City, Finney County, Kansas, are presented. All the results reported are organized chronologically according to the following order: (1) statistical analysis framework; (2) climate and water budget of growing season; (3) corn grain yield; (4) irrigation water productivity; (5) soil hydraulic function; and (6) relations between hydraulic indicators and crop response. Unless indicated otherwise, means are calculated based on 36 experimental plots, including 18 irrigated and 18 with irrigation deficits. All F-tests for the irrigation treatment effect are conducted on the Block × Irrigation interaction (df = 2) as a whole-plot error term. All main and interaction effects of amendment treatments are assessed against subplot error (df = 20). The effect is considered statistically significant if $\alpha = 0.05$ and marginally significant (†) if $0.05 \leq p < 0.10$.

4.1 Statistical Reporting Framework

The experiment was conducted according to the RCBD split-plot design with three blocks. Whole-plot treatments were irrigation (W100 and W50), and subplot treatments were factorial, consisting of biochar rate (0, 1, and 3.5 t ha^{-1}) and APSA-80 application (yes and no). Because of the error structure of the split-plot design, the effect of the irrigation treatment needs to be tested against the Block × Irrigation interaction effect (df = 2) rather than the subplot error (df = 20). Other effects must be tested against subplot error. This design arrangement allows us to avoid treating the 36 individual subplots as 36 different irrigation treatments.

4.2 Growing Season Climate and Water Budget

4.2.1 Seasonal Precipitation and Evapotranspiration

The growing season for corn in Garden City, Kansas (June 11 - November 6), is characterized by high evapotranspiration. The growing-season climate corresponds to a semi-arid regime typical of the southern High Plains region. Total precipitation for the season was 284.2 mm (11.19 inches). At the same time, the growing-season ET of alfalfa was 955.3 mm, and that of grass was 730.5 mm; both were much higher than precipitation (see Table 4.1 and Figure 4.1). The month with maximum demand was July, when ET of alfalfa was 253.5 mm, while precipitation was only 48.8 mm. There were eight irrigation events from June 18 to August 23, 2025. In September, the precipitation was 115.1 mm—the highest for this month and 113.3% of the total deficit irrigation amount. This precipitation occurred during the R4-R6 grain-filling period and was a very important climatic factor. Source: Kansas Mesonet (2025); ET by FAO-56 Penman-Monteith (Allen et al., 1998).

Table 4.1. Monthly rainfall, reference evapotranspiration (grass reference crop and alfalfa reference crop).

Period	Precipitation (mm)	ET grass (mm)	ET alfalfa (mm)	Irrigation events	Notes
Jun 11–30	30.7	138.2	182.4	1	Planting: emergence Jun 18
July	48.8	199.6	253.5	4	Peak ET; VT–R2 critical period
August	63.0	167.1	214.1	3	Last irrigation: August 23
September	115.1	116.3	148.6	0	Post-irrigation; R4–R6; 113.3% of deficit total
October	26.7	96.0	137.7	0	Dry-down; physiological maturity
Nov 1–6	0.0	13.2	19.0	0	Hand harvest November 6–7
Season total	284.2	730.5	955.3	8	Jun 11 – Nov 6, 2025

4.2.2 Water Budget for Irrigation Treatments

The total amount of water applied per season depended on the irrigation method employed. Under W100 irrigation, total water use was 487.4 mm (203.2 mm from irrigation and 284.2 mm from precipitation), whereas under W50 irrigation, it was 385.8 mm (101.6 mm from irrigation and 284.2 mm from precipitation). As for the percentage contribution of precipitation to total water use, it was 58.3% for W100 irrigation and 73.7% for W50 irrigation. It shows that precipitation played an important role in the water budget in 2025. The contributions of both irrigation treatments to the total ET of ~625 mm were 77.9% and 61.7%, respectively.

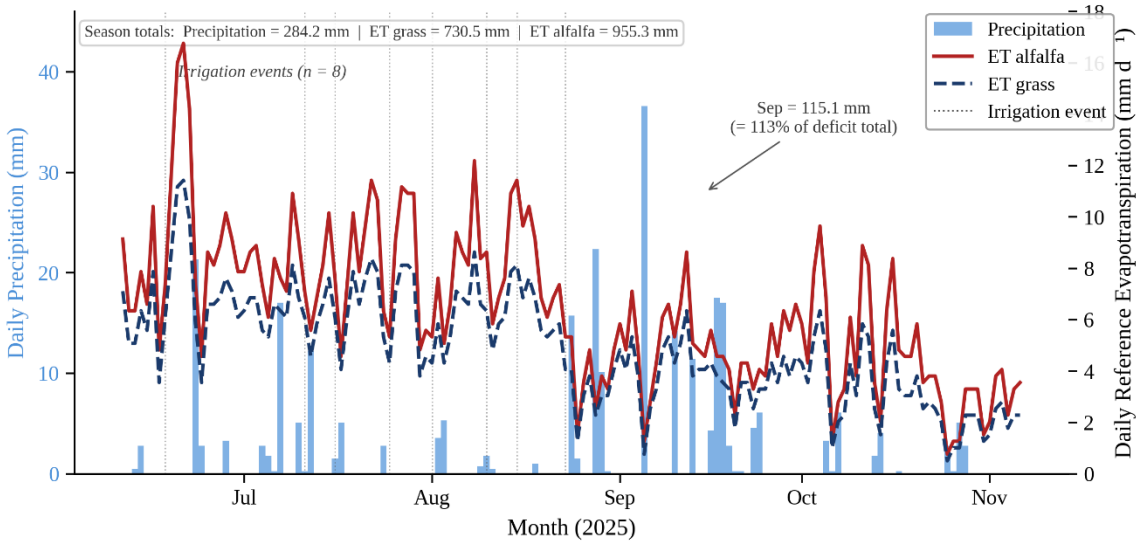


Figure 4.1 Daily precipitation (mm) and reference evapotranspiration (ET alfalfa and ET grass, mm d^{-1}) during the 2025 corn growing season (June 11–November 6, Garden City, Kansas).

4.3 Response of corn grain yield to irrigation and amendment treatments

Corn grain yield (adjusted to 15.5% moisture content) ranged from 167.4 to 237.5 bu/ac (10,773 to 14,935 kg/ha) and had a grand average of 198.6 bu/ac (12,461 kg/ha). Irrigation was the

principal contributor to grain yield. The impact of soil amendments was insignificant at $\alpha = 0.05$ during the first growing season.

4.3.1 Influence of irrigation on yield

The plots irrigated with W100 treatment gave an average grain yield of 205.92 bu/ac (12,926 kg/ha; SE = 3.45; 95% CI = ±14.85 bu/ac), while plots with W50 irrigation resulted in a grain yield of 191.36 bu/ac (12,012 kg/ha; SE = 3.45; 95% CI = ±14.85). The yield difference of 14.56 bu/ac corresponds to a 7.1% yield reduction under 50% deficit irrigation. Using the correct whole-plot error term, the result was not statistically significant. Nevertheless, this was a marginal effect ($F_{1,2} = 8.904$, $p = 0.0964$, †) that proves the conservativeness of the whole plot test, where only 3 blocks have been used. The critical value of F for $p = 0.05$ and $df = (1, 2)$ is 18.51. On the other hand, the result is significant in all three blocks in terms of the sign: Block 1 (203.99 vs. 196.81 bu/ac), Block 2 (212.36 vs. 188.58 bu/ac), and Block 3 (201.41 vs. 188.69 bu/ac), with W100 irrigation exceeding W50 in every block.

A 7.1% yield penalty under 50% W50 irrigation was lower than the 10-18% yield reductions described in the published High Plains literature (Rudnick et al., 2019; Klocke et al., 2011; Stone et al., 2008). This can be explained by two reasons: (1) rainfall in September 2025 equaled 115.1 mm after irrigation was stopped on August 23; hence, the availability of water during the R4-R6 period (stress-insensitive grain filling stage) was equal for both treatments; and (2) because of the restriction in well capacity, the full treatment met 78% of the evapotranspiration needs. Treatment means, SDs, and results of the statistical analysis are shown in Tables 4.3 and 4.4.

Table 4.2. Corn grain yields descriptive statistics by irrigation regime

Irrigation treatment	n	Mean (bu ac^{-1})	Mean (kg ha^{-1})	SD	SE	WP 95% CI (bu ac^{-1})
W100 (203.2 mm)	18	205.92	12926	13.35	3.45	± 14.85
W50 (101.6 mm)	18	191.36	12012	10.97	3.45	± 14.85
Difference (W100 – W50)	—	14.56	914	—	—	—

Table 4.3. Split-plot ANOVA for corn grain yield

Source of variation	Num. df	Den. df	F	p	Sig.
Block	2	—	—	—	—
Irrigation (whole-plot)	1	2	8.904	0.0964	†
Biochar	2	20	1.415	0.2641	NS
APSA-80	1	20	0.684	0.4170	NS
Biochar × APSA-80	2	20	0.858	0.439	NS
Irrigation × Biochar	2	20	2.581	0.0984	†
Irrigation × APSA-80	1	20	1.827	0.192	NS
Irrigation× Biochar × APSA-80	2	20	—	>0.40	NS

Note: Irrigation tested against Block × Irrigation error (MS = 214.357, df = 2). All other effects tested against subplot residual (MS = 128.436, df = 20). † $p < 0.10$; NS = not significant.

4.3.2 Yield Response to Amendments

The impact of biochar rates on corn grain yield was not significant ($F_{2,20} = 1.415$, $p = 0.2641$, NS). Marginal means are 0 t ha^{-1} = 195.3 bu ac^{-1}; 1 t ha^{-1} = 197.6 bu ac^{-1}; and 3.5 t ha^{-1} = 203.1 bu ac^{-1}, which shows a positive trend; however, it is not statistically significant, especially for the high rate of biochar and W100 irrigation (mean = 213.1 bu ac^{-1}). APSA-80 did not significantly affect yield ($F_{1,20} = 0.684$, $p = 0.4170$, NS). Irrigation × biochar interaction exhibited marginal significance ($F_{2,20} = 2.581$, $p = 0.0984$, †), indicating that the effect of biochar on yield could be slightly positive

only in full irrigation, but not in deficit irrigation. However, the trend has not reached the $\alpha = 0.05$ level in the season one data.

Table 4.4. Descriptive corn grain yield means (bu ac^{-1}) and standard deviations for all irrigation × biochar × APSA-80 treatment combinations, = 3 per combination.

Irrigation	Biochar	APSA-80	Yield (bu ac^{-1})	Yield (kg ha^{-1})	IWP (kg ha^{-1} mm^{-1})	SD	n
W100	0 t ha^{-1}	Without	208.64	13096	64.45	16.85	3
W100	0 t ha^{-1}	With	203.43	12769	62.84	6.56	3
W100	1 t ha^{-1}	Without	192.17	12062	59.36	11.50	3
W100	1 t ha^{-1}	With	205.05	12871	63.34	10.37	3
W100	3.5 t ha^{-1}	Without	204.47	12834	63.16	6.75	3
W100	3.5 t ha^{-1}	With	221.77	13921	68.51	14.70	3
W50	0 t ha^{-1}	Without	185.56	11647	114.64	16.27	3
W50	0 t ha^{-1}	With	183.49	11518	113.36	14.04	3
W50	1 t ha^{-1}	Without	197.51	12398	122.03	9.22	3
W50	1 t ha^{-1}	With	195.52	12273	120.80	7.06	3
W50	3.5 t ha^{-1}	Without	193.83	12167	119.75	5.65	3
W50	3.5 t ha^{-1}	With	192.23	12066	118.76	12.55	3

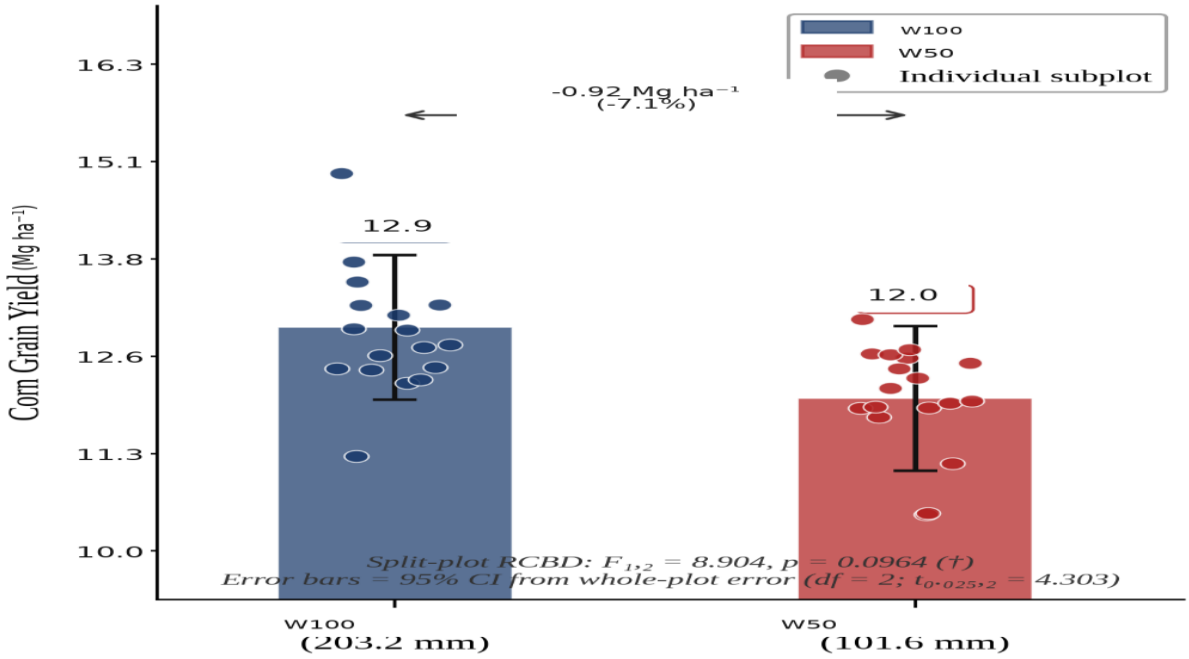


Figure 4.2 Corn grain yield (Mg ha^{-1}) as a function of irrigation treatment.

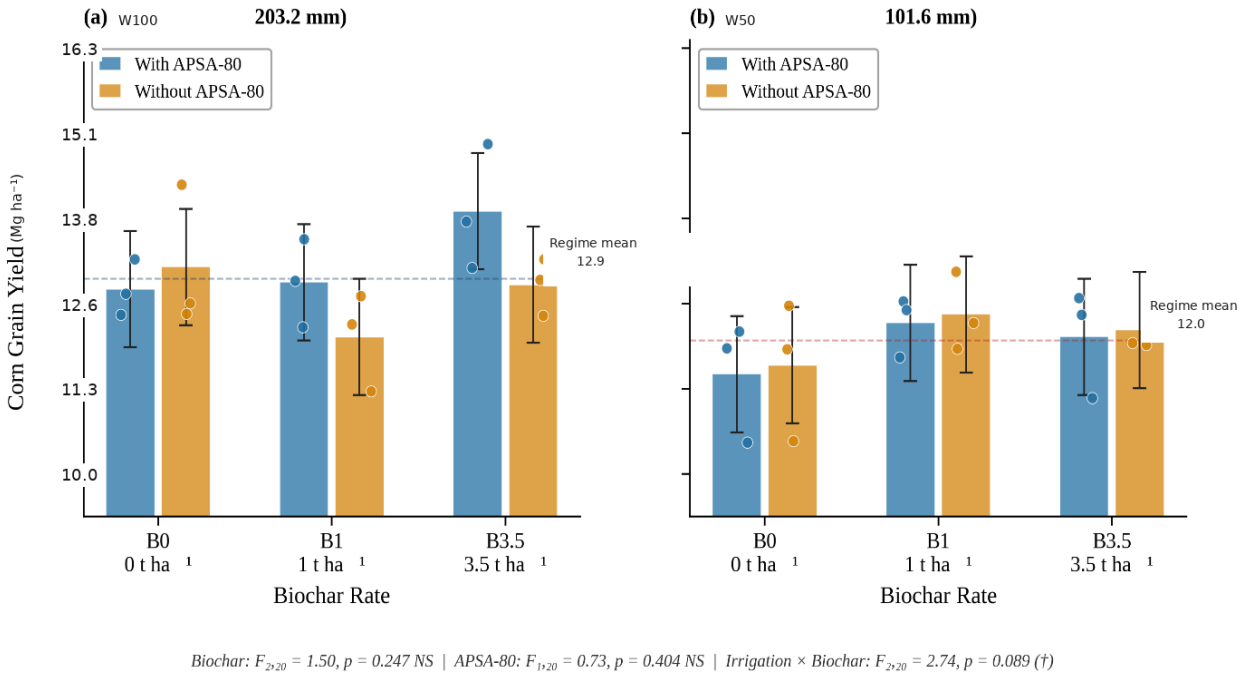


Figure 4.3 Effect of application rate of biochar and APSA-80 on corn grain yield (Mg ha $^{-1}$) using (a) W100 and (b) W50 irrigation methods

4.4 Irrigation Water Productivity and Total Water Productivity

There was a significant difference between irrigation water productivity (IWP = yield/irrigation amount) in different irrigation amounts. The W100 irrigation amount plots showed IWP as 63.61 kg ha^{-1} mm^{-1} (SE = 1.57; 95% CI = ±6.75), while the W50 irrigation amount plots had IWP as 118.22 kg ha^{-1} mm^{-1} (SE = 1.57; 95% CI = ±6.75), which is an improvement of 85.9% in IWP ($F_{1,2}$ = 606.31, p = 0.0016). This highly significant result clearly supports Hypothesis H2: a 50% reduction in the amount of irrigation water caused a proportionately much smaller yield reduction (7.1%), thus producing a considerably larger IWP. There is no block-by-irrigation interaction in IWP—in other words, this result holds across all three blocks. In terms of producer units, IWP values are about 63.61 and 118.22 kg ha^{-1} mm^{-1} for W100 and W50 irrigation, respectively.

Effects of the amendment on IWP are not significant (all $p > 0.10$). The ANOVA table of IWP is shown in Table 4.5.

Table 4.5. Split-plot ANOVA for irrigation water productivity (IWP, kg ha^{-1} mm^{-1})

Source	Num. df	Den. df	F (IWP)	p (IWP)	Sig.	F (TWP)	p (TWP)	Sig.
Irrigation	1	2	606.31	0.0016	**	65.51	0.0000	*
Biochar	2	20	1.407	0.268	NS	1.407	0.268	NS
APSA-80	1	20	0.144	0.709	NS	0.144	0.709	NS
Biochar × APSA-80	2	20	0.351	0.708	NS	0.351	0.708	NS
Irrigation × Biochar	2	20	2.387	0.118	NS	2.387	0.118	NS
Irrigation × APSA-80	1	20	1.016	0.326	NS	1.016	0.326	NS

4.5 Field-Saturated Hydraulic Conductivity (K_{fs})

4.5.1 Pre-Treatment Baseline Equivalence

K_{fs} pre-treatment analysis established the statistical equivalence of the W100- and W50-irrigation plots (W100: 0.000338 cm s^{-1}; W50: 0.000365 cm s^{-1}; $F_{1,2} = 0.029$ for baseline; see Table 4.8). The pre-treatment baseline VWC showed statistical equivalence (W100: 22.38%; W50: 22.76%; $F_{1,2} = 0.114$, $p = 0.7674$, NS). Such results indicate that the design is randomized; hence, any difference in post-treatment KFs can be attributed to treatment effects.

Across all 36 subplots, K_{fs} decreased from a pre-treatment mean of 0.3517×10^{-3} cm s^{-1} to 0.3044×10^{-3} cm s^{-1}, yielding an average K_{fs} fold change of 0.870 (13%). K_{fs} dropped in 34 of 36 subplots, while in the remaining two subplots under deficit irrigation, there was a slight increase of less than 3%. The almost universal drop in K_{fs} values can be explained by the process of formation of surface seal and dispersion of soil under irrigation conditions (Levy & Mamedov, 2002).

Table 4.6. Pre-treatment and post-treatment K_{fs} summary and ANOVA for K_{fs} fold-change

Metric	W100 irrigation	W50 irrigation	All plots
Pre-treatment K_{fs} (cm s^{-1})	0.000338	0.000365	0.000352
Post-treatment K_{fs} (cm s^{-1})	0.000293	0.000315	0.000304
Fold-change (post/pre)	0.865 (SE = 0.029)	0.875 (SE = 0.022)	0.870
% K_{fs} change	-13.5%	-12.5%	-13.0%
Plots with K_{fs} decline.	—	—	34/36 (94.4%)
n	18	18	36

4.5.2 APSA-80 Effects on K_{fs}: Irrigation Interaction

There was no effect of irrigation on the fold change in K_{fs} ($F_{1,2} = 0.029$, $p = 0.8812$, NS; Table 4.7). The interaction of irrigation and APSA-80 on the fold change of K_{fs} was a marginal effect ($F_{1, 20} = 3.997$, $p = 0.0593$, †; Table 4.7), while the main effect of APSA-80 was insignificant ($F_{1, 20} = 2.219$, $p = 0.1519$, NS). As seen from the pattern of means, this interaction depends on the following: the presence of APSA-80 caused a higher mean fold change (0.921) in comparison to no-APSA (0.809) for the case of W100 irrigation, meaning that APSA-80 prevented a greater reduction of K_{fs} because of higher water per event (25.4 mm $event^{-1}$). Under W50 irrigation, both treatments had similar fold changes (0.867 vs. 0.883), corresponding to a lower per-event water volume (12.7 mm $event^{-1}$), which causes less surface hydraulic disturbance (Levy & Mamedov, 2002; Kostka, 2000). There was no influence of biochar on the fold change of K_{fs} ($F_{2, 20} = 0.716$, $p = 0.5010$, NS) according to Hypothesis H_4, considering the assumption that fine-textured soils cannot be hydraulically affected by biochar during the first season at a rate of less than 5 t ha^{-1} (Blanco-Canqui, 2017).

Table 4.7. ANOVA for K_{fs} fold-change (post-treatment K_{fs} / baseline K_{fs})

Source of variation	Num. df	Den. df	F	p	Sig.
Irrigation (whole-plot)	1	2	0.029	0.8812	NS
Biochar	2	20	0.716	0.501	NS
APSA-80	1	20	2.219	0.152	NS
Biochar × APSA-80	2	20	0.910	0.418	NS
Irrigation × Biochar	2	20	0.397	0.678	NS
Irrigation × APSA-80	1	20	3.997	0.0593	†
Irrigation× Biochar × APSA-80	2	20	—	>0.20	NS

Table 4.8. K_{fs} fold-change means by Irrigation × APSA-80 combinatioN. n = 9 per combination; 95% CI from subplot residual (df = 20; $t_{0.025,20} = 2.074$).

Irrigation	APSA-80	K_{fs} fold change (mean)	95% CI	Interpretation
W100	With APSA-80	0.921	±0.074	Least K_{fs} decline
W100	Without APSA-80	0.809	±0.074	Greatest K_{fs} decline
W50	With APSA-80	0.867	±0.074	No APSA-80 benefit
W50	Without APSA-80	0.883	±0.074	Similar without surfactant
Irrigation × APSA-80:	$F_{1,20} = 3.997$	p = 0.0593 (†)		

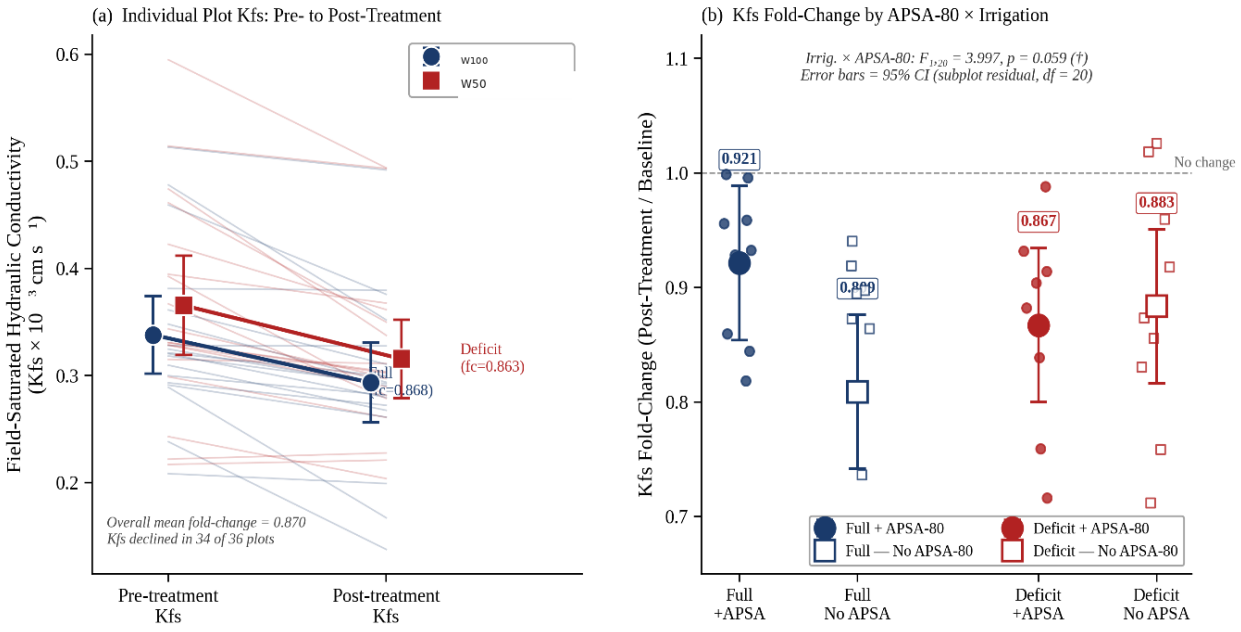


Figure 4.4 (a) Individual plot K_{fs} (× 10^{-3} cm s^{-1}) from pre-treatment to post-treatment, with colored lines indicating irrigation regime assignment. Large symbols show irrigation regime means ± 95% CI; small lines show individual subplots. (b) K_{fs} fold-change (post/baseline) by APSA-80 × irrigation treatment, with individual subplot observations.

4.6 Volumetric Water Content Dynamics

4.6.1 Baseline and Post-Irrigation VWC

The VWC values measured before the application of any treatments showed statistically equal means in percentage terms for the irrigation treatments (22.38% and 22.76%; $F_{1,2} = 0.114$, $p = 0.7674$, NS), thereby confirming hydraulic equivalence before treatment application. The VWC values measured 24 hours after the irrigation procedure were also very similar for the W100 and W50 irrigation treatments (32.46% and 32.57%), implying that the irrigation volume filled the soil volume at a depth of 10 cm to nearly saturated levels. Major differences in VWC values detected between treatments were related to the dynamics of depletion between events, not to the post-irrigation recharge amount.

4.6.2 Pre-Irrigation Trough VWC and Between-Event Depletion

The mean value of VWC at the trough before irrigation, averaged over the four monitored growth stage windows (V6-V7, V8-V9, V10-V11, and VT), was 29.58% and 27.34% in the W100 and W50 treatment plots, respectively, and produced a directional effect of 2.25 pp, which was statistically insignificant ($F_{1,2} = 5.672$, $p = 0.1402$, NS; Table 4.9). The same pattern was shown over all four monitored growth-stage intervals (Figure 4.5). The mean drawdown of VWC between events (VWC 24 hours after irrigation minus VWC at the trough) was 2.88 pp and 5.23 pp in the full and deficit plots, respectively, and produced an 81.6% greater depletion between events under deficit conditions. However, this effect was statistically insignificant at the plot level ($F_{1,2} = 3.426$, $p = 0.2054$, NS; Figure 4.6). VWC at harvest was higher in the W100 irrigation treatment plots (29.31% vs. 27.84%; $F_{1,2} = 9.135$, $p = 0.0943$, †). The spatial effects within blocks were statistically significant for post-irrigation VWC and trough VWC ($p < 0.05$). All amendments on the VWC were insignificant (all $p > 0.10$).

Table 4.9. VWC response means irrigation F-tests (whole-plot error, df = 2)

VWC metric (10 cm depth)	W100(%)	W50(%)	Diff. (pp.)	$F_{1,2}$	p	Sig.
Baseline (pre-treatment)	22.38	22.76	+0.38	0.17	0.686	NS
Post-irrigation 24 h mean	32.46	32.57	+0.11	—	—	NS
Trough—V6–V7	29.61	27.32	−2.29	—	—	Dir.
Trough—V8–V9	29.49	27.44	−2.05	—	—	Dir.
Trough—V10–V11	29.73	27.42	−2.31	—	—	Dir.
Trough—VT	29.51	27.18	−2.33	—	—	Dir.
Trough the mean	29.58	27.34	−2.25	5.672	0.1402	NS
Drawdown means	2.88	5.23	+2.35	3.426	0.2054	NS
VWC at harvest	29.31	27.84	−1.47	9.135	0.0943	†

† $p < 0.10$; NS = not significant. Dir. = descriptive stage-level means only; no F-test conducted at individual growth stage level because stage measurements are correlated repeated observations

within each plot (Girden, 1992). The formal F-test used the plot-level mean across all four stages.

Table 4.10. Between-event VWC drawdown (pp) at 10 cm depth by growth stage and irrigation treatment, n = 18 per treatment × stage.

Growth stage	Irrigation	n	Mean drawdown (pp)	SE	95% CI
V6–V7	W100	18	3.00	0.36	2.30–3.71
V6–V7	W50	18	5.23	0.45	4.36–6.10
V8–V9	W100	18	3.01	0.41	2.20–3.82
V8–V9	W50	18	5.15	0.46	4.25–6.06
V10–V11	W100	18	2.69	0.35	2.01–3.36
V10–V11	W50	18	5.25	0.49	4.29–6.22
VT	W100	18	2.82	0.36	2.12–3.53
VT	W50	18	5.29	0.44	4.43–6.15

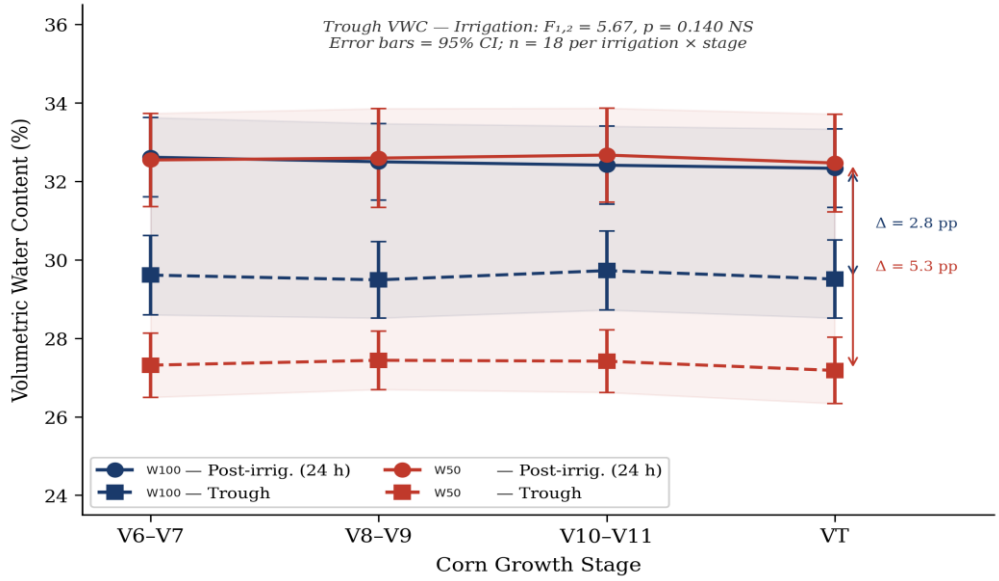


Figure 4.5. Volumetric water content (VWC, %) measured 24 h after irrigation (solid lines) and at the pre-irrigation trough (dashed lines) by corn growth stage and irrigation treatment.

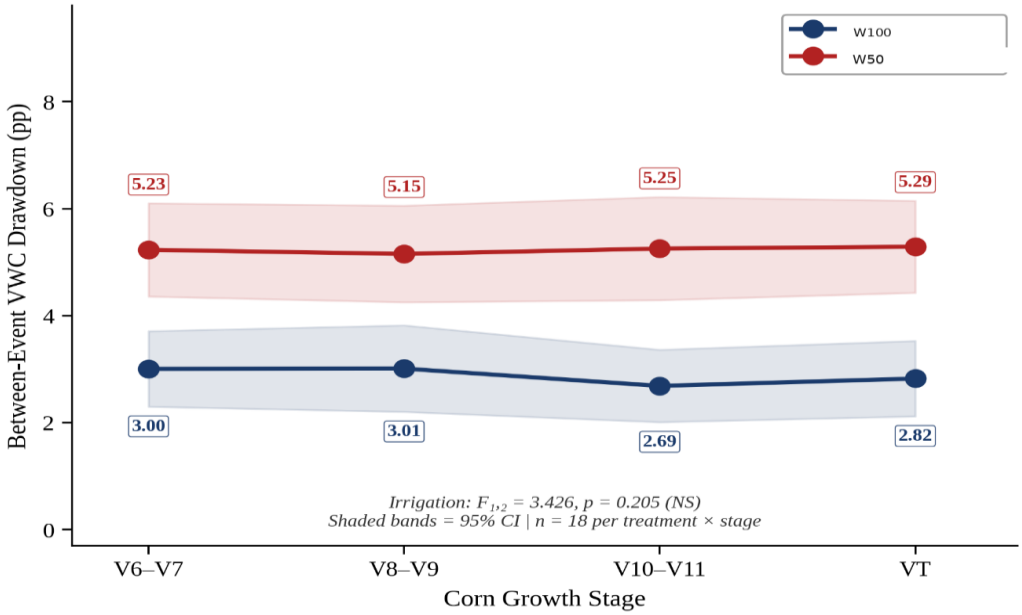


Figure 4.6. Between-event soil water drawdown (pp = post-irrigation VWC minus trough VWC) by corn growth stage and irrigation treatment.

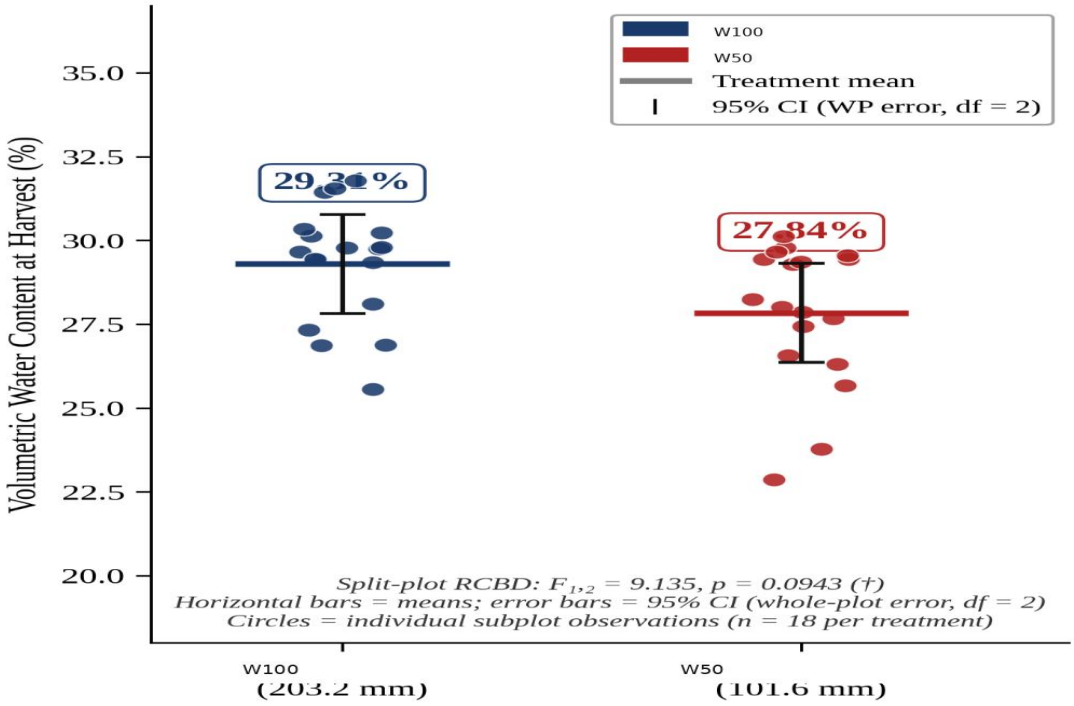


Figure 4.7. Volumetric water content (VWC, %) at corn harvest (November 6–7, 2025) by irrigation treatment.

4.7 Correlations Between Soil Hydraulics and Grain Yield

The average value of pre-irrigation trough VWC is significantly and positively correlated with corn grain yield (ρ = +0.377, p = 0.0235), which means that the higher moisture content of soil before each irrigation event corresponds to the higher yield, confirming the hypothesis about the importance of between-event soil moisture content for the prediction of the variability of experiment-based yield. Also, the VWC value at harvest is significantly correlated with grain yield (ρ = +0.338, p = 0.0439*)*. A significant negative correlation between VWC drawdown between events and grain yield has been detected (ρ = -0.314, p = 0.0624, †), which means that plots with higher VWC drop between irrigation events are characterized by lower yield. Post-irrigation VWC 24 hours after irrigation hasn't shown any significant correlation with grain yield (ρ = +0.075, NS). It can be considered agronomically reasonable because post-irrigation VWC is nearly the same

across all treatment options. Also, post-treatment K_{fs} (ρ = +0.048, p = 0.7827, NS) and K_{fs} fold-change (ρ = +0.067, p = 0.6959, NS) have not shown any significant correlation with grain yield. Spearman correlations between soil hydraulic property indicators within the plot and corn grain yield (n = 36) are presented in Table 4.11 and Figure 4.8.

Table 4.11. Spearman rank correlations (ρ) between plot-level hydraulic indicators and corn grain yield (n = 36 plots), SWREC Garden City, Kansas, 2025. NS = not significant; † p < 0.10; * p < 0.05.

Hydraulic indicator	Spearman ρ	p-value	Sig.	Interpretation
VWC 24 h post-irrigation (%)	+0.075	0.665	NS	Post-event VWC equivalent; not predictive
Pre-irrigation trough VWC (%)	+0.377	0.023	*	Higher soil water before event → higher yield
Between-event drawdown (pp)	-0.314	0.062	†	Less depletion → higher yield
VWC at harvest (%)	+0.338	0.044	*	Higher end-of-season VWC → higher yield
Post-treatment K_{fs} (cm s^{-1})	+0.048	0.783	NS	Reduced K_{fs} still adequate; not predictive.
K_{fs} fold-change (post/baseline)	+0.067	0.696	NS	Seasonal KFs change, not predictive.

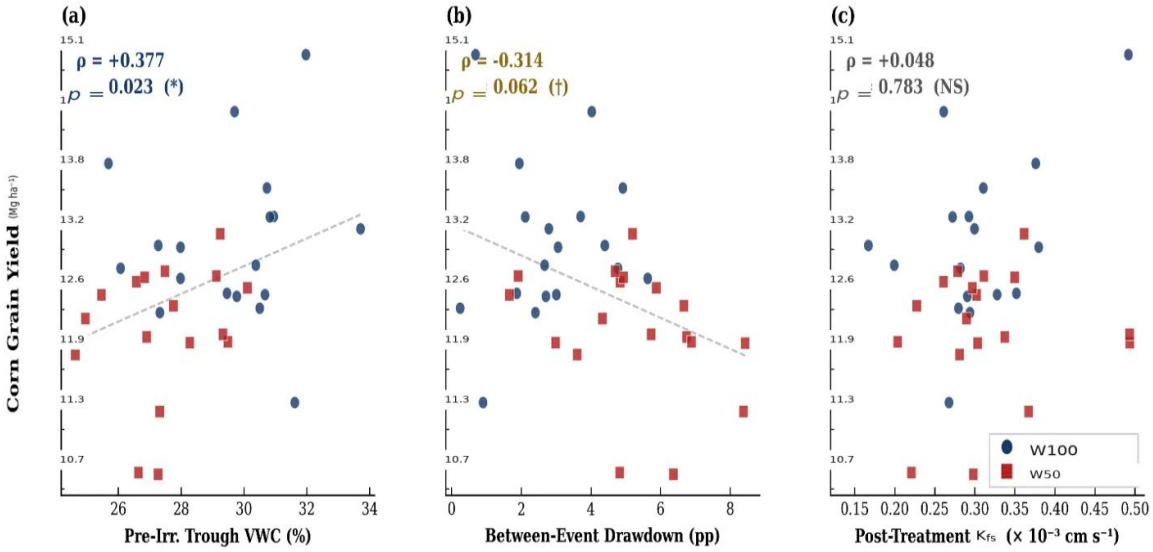


Figure 4.8. Spearman rank scatter plots: (a) pre-irrigation trough VWC (%) vs. yield (ρ = +0.377, p = 0.024, *); (b) between-event drawdown (pp) vs. yield (ρ = −0.314, p = 0.062, †); (c) post-treatment Kfs (cm s⁻¹) vs. yield (ρ = +0.048, NS).

4.8 Summary of Major Results

Four key findings were revealed during the 2025 field experiment. First, W50 irrigation reduced seasonal irrigation by 50%, although this irrigation had a significant negative effect on mean grain yield, causing a reduction of 7.1% (marginal trend, p = 0.096, †; whole-plot test with 3 replicate blocks*).* Second, IWP exhibited an 85.9% increase in response to W50 irrigation (p = 0.002, *). It was one of the most significant and statistically robust effects among the agronomic treatments used in this experiment. Third, all 36 plots had a seasonal reduction in K_{fs}, and APSA-80 tended to reduce it in W100 irrigation significantly more than in deficit irrigation (Irrigation × APSA-80: p = 0.059, †). Fourth, there was a significant relation between VWC trough and harvest VWC and yield ($p < 0.05$) but not surface K_{fs}. It indicates that soil-water dynamics are the key hydraulic parameter in this case of a linear irrigation system.

Chapter 5 - Discussion, Conclusion, and Implications

5.1 Yield Response to Deficit Irrigation (Objective 1, H1)

A 50% W50 irrigation lowered corn grain yield by 7.1% (12,925..60 vs. 12,011.67 kg ha^{-1}; $F_{1,2}$ = 8.904, p = 0.0964, †), confirming the directional prediction of H1, though the conservative whole-plot test with df = 2 precluded statistical significance at α = 0.05. Importantly, this negative effect on yield was consistently observed across all three replicated blocks, and this agronomically relevant observation should be given due weight, given the conservative nature of the F-test in whole-plot designs with just three blocks (Gomez & Gomez, 1984).

This 7.1% yield reduction falls within the 10–18% deficit-irrigation impact reported in the High Plains by Rudnick et al. (2019) and is about 15% in western Kansas, according to Klocke et al. (2011). There are two reasons why this reduction was relatively small: (1) rainfall in September 2025 post-irrigation (115.1 mm = 113.3% of the deficit season total allocation) made the water availability for the R4–R6 stage equal among treatments, while this period had much lower sensitivity to the water deficiency than the VT–R2 stage (NeSmith & Ritchie, 1992); and (2) the capacity limit of the well meant that the W100 treatment had ET_c replaced by approximately 78%. Araya et al. (2021) similarly pointed out in western Kansas that a well-capacity limit can reduce the yield penalty associated with deficit irrigation.

5.2 Irrigation Water Productivity (Objective 2, H2)

IWP was 85.9% greater with W50 irrigation ($F_{1,2}$ = 606.31, p = 0.0016)—the main and most statistically significant agronomic result of this study and strong evidence for H_2. With a 50% decrease in pumped groundwater quantity, yield decreased by only 7.1%, resulting in a significantly higher yield per unit of water extracted. The W50 irrigation strategy implies that, for

producers in Groundwater Management District No. 3, corn yield is about 1.86 times greater per millimeter of pumped water (English, 1990; Molden et al., 2010; Steiner et al., 2021). This result was supported by Igwe et al. (2025), who found that deficit irrigation practices can sustain acceptable crop yields and dramatically reduce groundwater use under severe climatic conditions. At the regional scale, according to Whittemore et al. (2023), southwest Kansas aquifers continue to decrease at a rate of about 0.9 m yr^{-1}. IWP values obtained in this research demonstrate the potential to dramatically reduce the extraction rate without affecting yield under favorable precipitation conditions.

The comparison of IWP superiority (85.9%) with TWP superiority (17.4%) provides insight into the influence of precipitation. If 284.2 mm of precipitation is treated as equivalent across both treatments and placed in the denominator, the superiority of the efficiency drops sharply. IWP is the right indicator for groundwater management (Zwart & Bastiaanssen, 2004; Molden et al., 2010).

5.3 Soil Hydraulic Function—K_{fs} (Objective 3, H3)

The near-consistent reduction in K_{fs} (34/36 plots; fold-change = 0.870) indicates the susceptibility of the Ulysses silt loam surface to progressive surface structure alteration through repetitive irrigation-induced wetting and drying cycles, which is a surface seal creation mechanism through the effect of irrigation water application to the soil surface, fine particle movement, and interaggregate pore clogging (Levy & Mamedov, 2002). The significance of K_{fs} reduction due to linear-move overhead irrigation is that infiltration of irrigation water into the soil decreases, leading to surface ponding when K_{fs} falls below the irrigation application rate.

The marginal interaction between irrigation and APSA-80 ($F_{1,20} = 3.997$, $p = 0.0593$, †) provides partial confirmation of H3. The APSA-80 showed significant buffering against the reduction of K_{fs} when applied with W100 irrigation (fold change 0.921 compared with 0.809 with the surfactant) but no buffering effect with W50 irrigation (0.867 compared with 0.883). This observation can be explained from a mechanical perspective because in the case of W100 irrigation, the application of 25.4 mm event^{-1} overhead imposes higher hydraulic energy on the soil surface and, consequently, creates better opportunities for the APSA-80 effect on improving the irrigation water infiltration uniformity (Kostka, 2000; Almaz et al., 2023). In the case of W50 irrigation, the low irrigation rate of 12.7 mm event^{-1} leads to less disruption of the soil surface, resulting in the limited effect of APSA-80.

The lack of any significant impact from biochar on K_{fs} in the first season strongly supports H4 and agrees with findings by Blanco-Canqui (2017) and Gelardi et al. (2021), who indicated that the hydraulic impact of biochar in fine-textured soils with applications of less than 5 t ha^{-1} requires more than one growing season to manifest itself. Similarly, Hassan et al. (2022), working in sandy loam soils near the Ulysses silt loam used in our experiment, also found a modest first-season response in K_{fs} at producer-level biochar rates.

It is worth noting that the multi-year trajectory of biochar's hydraulic effects, as documented in scientific literature, provides an important interpretative context for evaluating the first-season biochar impacts recorded in this research. Aller et al. (2018) investigated the effects of biochar amendments on soil quality and corn yield in the U.S. Midwest over several consecutive seasons. They found that improvements in soil physical properties, such as water retention and aggregate stability, became evident progressively and reached their highest magnitude in the third and fourth

years after biochar application. Moreover, Acharya et al. (2024) discussed the mechanistic basis of this phenomenon. It was found that three sequential steps should be followed by biochar to create a reliable hydraulic effect in fine-textured soils, namely, (1) the physical incorporation of biochar particles into the soil aggregate system due to repeated wetting, drying, and freeze-thaw cycles; (2) the chemical modification of biochar through interaction with soil organic matter and its wettability; and (3) the colonization of biochar pores by microorganisms, causing the change in biochar pore size distribution and water retention. None of these steps can occur within a single growing season at the 1 and 3.5 t ha^{-1} biochar application rates used in this research.

According to the findings of Jiang et al. (2024) in their global long-term assessment, the biochar crop yield response was 6.4% in year one but exceeded 14% by years four and five, demonstrating the significance of multiyear evaluation for proper biochar effect assessment. Thus, the insignificant effects of biochar on K_{fs}, VWC, and yield observed in the current research do not indicate the amendment's ineffectiveness in the ecosystem under consideration; rather, they suggest that the biochar integration process is still in its early stages. The trends of slight increases in VWC trough and yield under the 3.5 t ha^{-1} rate in both irrigation treatments correspond to the first stage of the multi-year trajectory described by Jiang et al. (2024) and Acharya et al. (2024).

5.4 VWC Dynamics (Objective 3, continued)

The trends for VWC are unambiguous and consistently directional across all four growth stages. No irrigational effects on the VWC attained statistical significance at $\alpha=0.05$ using the conservative whole-plot test because of the inherent power limitation that exists in the 2df whole-plot error term when there are only three blocks for replication (Gomez & Gomez, 1984). However,

all irrigation effects on the VWC were always directional during all four growth phases. The 81.6% greater VWC drawdown between events at 10 cm depth for the deficit irrigation (5.23 vs. 2.88 pp) is the hydraulic manifestation of decreased overhead application volumes per event, resulting in greater depletion of soil water between events, which is the physical process linking deficit irrigation to greater crop water stress (Ritchie, 1981).

5.5 Hydraulic-Yield Relationships (Objectives 4 and 5, H5)

The Spearman correlation results support hypothesis H5. Pre-irrigation VWC at a depth of 10 cm (ρ = +0.377, p = 0.023) and VWC at harvest (ρ = +0.338, p = 0.044) have shown significant positive correlations with yield. The drawdown between events has shown a weak negative correlation (ρ = -0.314, p = 0.062). All three significantly correlated VWC parameters describe the same hydraulic process and show that between-event root-zone water storage is the pathway through which irrigation management influences crop yield performance. According to Li et al. (2016), management-induced changes in soil water dynamics have become the key factor explaining the variance in IWP in semi-arid irrigated regions.

Post-treatment K_{fs} value (ρ = +0.048, p = 0.783, NS) did not correlate significantly with yield. However, it is a direct indicator of surface infiltration in the linear move overhead irrigation system used in this research. This means that the post-season decrease in K_{fs} values (average K_{fs} = 0.000304 cm/s; fold change = 0.870) was sufficient to provide adequate irrigation without yield-reducing water ponding and surface runoff during these treatments. The lack of a K_{fs}-yield correlation indicates that between-event root-zone water storage, as described by VWC dynamics, becomes the hydraulic process regulating yield performance. In other words, between-event water storage in the root zone became the agriculturally predominant hydraulic process regulating yield

performance in this setting, and any further efforts at instrumentation of this site should focus on using Acclima TDR probes in the root zone rather than measuring K_{fs}.

5.6 Practical Implications for Southwest Kansas

The 85.9% IWP is the most practically relevant result of this study. For a producer using a 100 ac-ft annual groundwater allocation under Kansas Groundwater Management District (GMD) No. 3 management criteria, corn yield does not increase per se, but for equal water applied, IWP of W50 is higher. Deficit irrigation was listed by Steiner et al. (2021) as the most readily actionable water conservation strategy in Kansas, and this IWP evidence helps substantiate that claim under linear-move overhead irrigation conditions at SWREC. Furthermore, Igwe et al. (2025) found that this strategy remained viable even under increasingly extreme climatic conditions, lending credence to its long-term viability.

In the case of the IWP improvement found in this study, the economic implications can be clearly explained using the water-to-income nexus, which guides producers' decisions in the Ogallala area. Araya et al. (2019) calculated the economic water productivity of irrigated crops in the Ogallala Aquifer region. They showed that although irrigated corn yields higher economic water productivity than alternative crops, its advantage quickly fades as water extraction costs increase due to aquifer depletion. Therefore, the increase in economic water productivity in this case will positively affect producers' economic performance.

Additionally, Araya et al. (2019) showed that the economic value of water is the greatest for corn among irrigated crops in the Ogallala region and is higher than for grain sorghum, wheat, and alfalfa. Besides, as mentioned above, under allocation management, in accordance with the requirements of the Kansas GMD No. 3, producers' annual groundwater allocation is restricted.

The enhancement identified in the present research contributes to maximizing corn income per acre-foot of allocated groundwater, resulting in nearly the maximum corn income from a fixed water quantity. It should be noted that the 85.9% increase for IWP can be regarded as a significant step towards maximizing the economic effectiveness of water extraction in this area, given the legislative basis provided by Kansas water laws and the goals of the Groundwater Management District No. 3 allocation management.

The marginal irrigation × APSA-80 K_{fs} interaction ($p = 0.059$, †) indicates that there is practical value in using APSA-80 soil conditioning for soil hydraulic maintenance under conditions of linear move overhead irrigation: APSA-80 is likely most effective in preserving K_{fs} under full irrigation (25.4 mm event^{-1}) conditions when overhead irrigation loading is greatest and seal formation is fastest. Producers with full-irrigation capacity looking to maintain K_{fs} during the season and avoid irrigation uniformity losses from K_{fs} reductions will likely see better results with APSA-80 than deficit producers will.

5.7 Limitations

- Whole-plot power of statistical test: For three replicates, the whole-plot error has df = 2, where $F > 18.51$ is required for $p < 0.05$. The effect of irrigation on yield and VWC is likely not statistically significant.
- Single VWC level at 10 cm: Sensors placed at the 10 cm depth level measure soil water dynamics in the near-surface soil. Using sensors at three soil depths (10, 30, and 45 cm) would help elucidate the root zone's response to irrigation events.

- One growing season: The data obtained in the first year represent pre-equilibrium conditions. Biochar effects will build up through several years (Blanco-Canqui, 2017; Gelardi et al., 2021).
- Precipitation in September 2025: Post-irrigation September precipitation of 115.1 mm decreased the difference between treatments in the late growing season. A drier year is likely to increase the yield gap by 10-18% (Rudnick et al., 2019).
- Depth of K_{fs} measurements: The measurements of K_{fs} were conducted for a 10 cm depth of the soil layer (ring insertion). Deeper measurements would provide complementary information about the hydraulic properties of the root zone.

5.8 Recommendations for Future Research

- Continue the experiment through ≥3 additional seasons (2026–2028) to understand the multi-seasonal dynamics of the biochar hydraulic and yield trajectories under linear move irrigation treatments.
- Add more blocks (four to five) to increase the power of statistical analysis in whole plots for the effect of irrigation.
- Deploy Acclima TDR probes at 10, 30, and 45 cm depths to develop the complete profile of VWC in the root zone to understand the dynamics of near-surface and deep-root-zone water dynamics.
- Analyze the significance of the irrigation × APSA-80 K_{fs} interaction in multiple seasons to confirm that this interaction is significant and whether APSA-80 is a viable option for hydraulic improvement in a higher irrigated system.

- Extend deficit irrigation × amendment experiments to 2026 field experiments in SWREC loamy sand fields.
- Carry out an economic analysis by converting IWP and yield results into economic benefit per acre-foot of groundwater allocation.

5.9 Conclusions

This first-season field experiment at SWREC, Garden City, Kansas, in 2025 produced five primary conclusions:

1. A 50% decrease in irrigation water applied through a linear move overhead irrigation system led to a 7.1% decrease in corn grain yield (205.92 to 191.36 bu ac^{-1}; $F_{1,2} = 8.904$, $p = 0.0964$, †). This decrease is consistent with the published 10–18% reduction in corn yield due to reduced irrigated water reported for the High Plains region (Rudnick et al., 2019) and was modified by an additional 115.1 mm of precipitation received in September and by well capacity.

2. W50 irrigation increased IWP by 85.9% (118.22 vs. 63.61 kg ha^{-1} mm^{-1}; $F_{1,2} = 606.31$, $p = 0.0016$, **)—the main result of this experiment. A 50% decrease in extracted water resulted in only a 7.1% decrease in yield, providing evidence for the viability of deficit irrigation as a means of improving groundwater extraction efficiency under Ogallala allocation constraints (Steiner et al., 2021; Whittemore et al., 2023; Igwe et al., 2025).

3. Seasonal K_{fs} values decreased in 34/36 plots (mean fold-change = 0.870; 13.0% decrease), as would be expected due to progressive surface seal formation in response to repeated overhead irrigation events. APSA-80 was able to mitigate this effect under W100 irrigation (ratio 0.921 compared to 0.809; Irrigation × APSA: $F_{1,20} = 3.997$, $p = 0.0593$, †) as was expected because the

mechanism according to which the surfactant is most effective in reducing the formation of surface seals is when the load of water applied per application is at its maximum (Kostka, 2000; Almaz et al., 2023). Biochar had no significant impact on any variable, thus confirming H4 (Blanco-Canqui, 2017; Gelardi et al., 2021).

4. Pre-irrigation trough soil moisture content at 10 cm depth ($\rho = +0.377$, $p = 0.023$) and VWC at harvest ($\rho = +0.338$, $p = 0.044$) were significant positive predictors of yield, validating H5. There is no effect of surface K_{fs} on yield ($\rho = +0.048$, NS), which means that the reduced levels of K_{fs} in the soil at the end of the season were adequate to support the irrigation levels.

5. The first-season data collection provides the basis for multi-season analysis of the effects of amendments and deficit irrigation management at SWREC, Garden City, Kansas, using linear move overhead irrigation systems.

In summary, 50% deficit irrigation through linear move overhead irrigation is a scientifically substantiated, agronomically feasible, and practical method for conserving groundwater for irrigated corn in the semi-arid southwest Kansas region. Further, the use of APSA-80 warrants assessment as a soil-hydraulic modifier, especially under heavy overhead irrigation loads. Moreover, biochar at field-realistic rates needs to be assessed over multiple years, and VWC measurements at rooting depths are more informative for crop yield prediction than K_{fs} measurements at the surface.

References

Abdoli, S., Asgari Lajayer, B., Bagheri Novair, S., & Price, G. W. (2025). Unlocking the Potential of Biosurfactants in Agriculture: Novel Applications and Future Directions. *Sustainability*, *17*(5), 2110. https://doi.org/10.3390/su17052110

Acharya, B. S., Dodla, S., Wang, J. J., Pavuluri, K., Darapuneni, M., Dattamudi, S., Maharjan, B., & Kharel, G. (2024). Biochar impacts on soil water dynamics: Knowns, unknowns, and research directions. *Biochar*, *6*(1), 34. https://doi.org/10.1007/s42773-024-00323-4

Adekiya, A. O., Agbede, T. M., Olayanju, A., Ejue, W. S., Adekanye, T. A., Adenusi, T. T., & Ayeni, J. F. (2020). Effect of Biochar on Soil Properties, Soil Loss, and Cocoyam Yield on a Tropical Sandy Loam Alfisol. *The Scientific World Journal*, *2020*, 9391630. https://doi.org/10.1155/2020/9391630

Allen, R. G. & Food and Agriculture Organization of the United Nations (Eds.). (1998). *Crop evapotranspiration: Guidelines for computing crop water requirements*. Food and Agriculture Organization of the United Nations.

Aller, D. M., Archontoulis, S. V., Zhang, W., Sawadgo, W., Laird, D. A., & Moore, K. (2018). Long-term biochar effects on corn yield, soil quality, and profitability in the US Midwest. *Field Crops Research*, *227*, 30–40. https://doi.org/10.1016/j.fcr.2018.07.012

Anandhi, A. (2016). Growing degree days—Ecosystem indicator for changing diurnal temperatures and their impact on corn growth stages in Kansas. *Ecological Indicators*, *61*, 149–158. https://doi.org/10.1016/j.ecolind.2015.08.023

Araya, A., Kisekka, I., Lin, X., Vara Prasad, P. V., Gowda, P. H., Rice, C., & Andales, A. (2017). Evaluating the impact of future climate change on irrigated maize production in Kansas. *Climate Risk Management*, *17*, 139–154. https://doi.org/10.1016/j.crm.2017.08.001

Araya, A., Gowda, P. H., Golden, B., Foster, A. J., Aguilar, J., Currie, R., Ciampitti, I. A., & Prasad, P. V. V. (2019). Economic value and water productivity of major irrigated crops in the Ogallala aquifer region. *Agricultural Water Management*, *214*, 55–63. https://doi.org/10.1016/j.agwat.2018.11.015

Araya, A., Prasad, P. V. V., Gowda, P. H., Sharda, V., Rice, C. W., & Ciampitti, I. A. (2021). Evaluating optimal irrigation strategies for maize in Western Kansas. *Agricultural Water Management*, *246*, 106677. https://doi.org/10.1016/j.agwat.2020.106677

Bates, D., Mächler, M., Bolker, B., & Walker, S. (2015). Fitting linear mixed-effects models using lme4. *Journal of Statistical Software*, *67*(1), 1–48. https://doi.org/10.18637/jss.v067.i01 Journal of Statistical Software

Báťková, K., Matula, S., Miháliková, M., Hrúzová, E., Abebrese, D. K., Serdar Kara, R., & Almaz, C. (2023). Prediction of saturated hydraulic conductivity Ks of agricultural soil using pedotransfer functions. *Soil and Water Research*, *18*(1), 25–32. https://doi.org/10.17221/130/2022-SWR

Blanco-Canqui, H. (2017). Biochar and Soil Physical Properties. *Soil Science Society of America Journal*, *81*(4), 687–711. https://doi.org/10.2136/sssaj2017.01.0017

Castellini, M., Ventrella, D., Giglio, L., Leogrande, R., Fornaro, F., & Niedda, M. (2014). *EFFECT OF BIOCHAR APPLICATION ON HYDRAULIC CONDUCTIVITY OF A CLAY SOIL*.

Edeh, I. G., Mašek, O., & Buss, W. (2020). A meta-analysis on biochar's effects on soil water properties—New insights and future research challenges. *Science of The Total Environment*, *714*, 136857. https://doi.org/10.1016/j.scitotenv.2020.136857

English, M. (1990). Deficit Irrigation. I: Analytical Framework. *Journal of Irrigation and Drainage Engineering*, *116*(3), 399–412. https://doi.org/10.1061/(ASCE)0733-9437(1990)116:3(399)

Feng, G. L., Letey, J., & Wu, L. (2002). The Influence of Two Surfactants on Infiltration into a Water-Repellent Soil. *Soil Science Society of America Journal*, *66*(2), 361–367. https://doi.org/10.2136/sssaj2002.3610

Gabhane, J. W., Bhange, V. P., Patil, P. D., Bankar, S. T., & Kumar, S. (2020). Recent trends in biochar production methods and its application as a soil health conditioner: A review. *SN Applied Sciences*, *2*(7), 1307. https://doi.org/10.1007/s42452-020-3121-5

Gelardi, D. L., Ainuddin, I. H., Rippner, D. A., Patiño, J. E., Abou Najm, M., & Parikh, S. J. (2021). Biochar alters hydraulic conductivity and impacts nutrient leaching in two agricultural soils. *SOIL*, *7*(2), 811–825. https://doi.org/10.5194/soil-7-811-2021

Girden, E. R. (1992). *ANOVA: Repeated Measures*. SAGE.

Graves, D. (2013). A Comparison of Methods to Apply Biochar into Temperate Soils. In *Biochar and Soil Biota*. CRC Press.

Gutierrez, M. M. (2025). *Biosurfactant and Soil Wetting Bacteria Amendments for Enhancing Water Retention in Agricultural Soils* [Ph.D., Kansas State University]. https://www.proquest.com/docview/3245399035/abstract/6DC0A25892594588PQ/1

Gutierrez, M. M., Cameron-Harp, M. V., Chakraborty, P. P., Stallbaumer-Cyr, E. M., Morrow, J. A., Hansen, R. R., & Derby, M. M. (2022). Investigating a microbial approach to water conservation: Effects of Bacillus subtilis and Surfactin on evaporation dynamics in loam and sandy loam soils. *Frontiers in Sustainable Food Systems*, *6*. https://doi.org/10.3389/fsufs.2022.959591

Gutierrez, M. M., Liu, S. C., Dip, S. A., Hettiarachchi, G. M., Derby, M. M., & Hansen, R. R. (2025). Impact of soil texture on biosurfactant-mediated soil wetting and water retention. *Agricultural & Environmental Letters*, *10*(2), e70043. https://doi.org/10.1002/ael2.70043

Haacker, E. M. K., Kendall, A. D., & Hyndman, D. W. (2016). Water Level Declines in the High Plains Aquifer: Predevelopment to Resource Senescence. *Groundwater*, *54*(2), 231–242. https://doi.org/10.1111/gwat.12350

Han, M., Zhang, J., Zhang, L., & Wang, Z. (2023). Effect of biochar addition on crop yield, water and nitrogen use efficiency: A meta-analysis. *Journal of Cleaner Production*, *420*, 138425. https://doi.org/10.1016/j.jclepro.2023.138425

Hassan, O., Ahmad, K., Hassan, T. S., & Hossein, S. (2022). *Biochar application impacts water infiltration rate into soil and field saturation hydraulic conductivity of sandy loam soil*. *16*(144), 103–112.

He, P., Liu, Y., Shao, L., Zhang, H., & Lü, F. (2018). Particle size dependence of the physicochemical properties of biochar. *Chemosphere*, *212*, 385–392. https://doi.org/10.1016/j.chemosphere.2018.08.106

Igwe, K., Onyekwelu, I., & Sharda, V. (2025). Adaptation strategies for deficit irrigation management under extreme climate conditions. *Agricultural Water Management*, *313*, 109506. https://doi.org/10.1016/j.agwat.2025.109506

Jeffery, S., Abalos, D., Spokas, K. A., & Verheijen, F. G. A. (2015). Biochar effects on crop yield. In *Biochar for Environmental Management* (2nd ed.). Routledge.

Jiang, Y., Li, T., Xu, X., Sun, J., Pan, G., & Cheng, K. (2024). A global assessment of the long-term effects of biochar application on crop yield. *Current Research in Environmental Sustainability*, *7*, 100247. https://doi.org/10.1016/j.crsust.2024.100247

Kang, M. W., Yibeltal, M., Kim, Y. H., Oh, S. J., Lee, J. C., Kwon, E. E., & Lee, S. S. (2022). Enhancement of soil physical properties and soil water retention with biochar-based soil

amendments. *Science of The Total Environment*, *836*, 155746. https://doi.org/10.1016/j.scitotenv.2022.155746

Kansas Mesonet. (2025). Retrieved June 28, 2026, from https://mesonet.k-state.edu/

Kostka, S. J. (2000). Amelioration of water repellency in highly managed soils and the enhancement of turfgrass performance through the systematic application of surfactants. *Journal of Hydrology*, *231–232*, 359–368. https://doi.org/10.1016/S0022-1694(00)00208-0

Kukal, M. S., & Irmak, S. (2018). Climate-Driven Crop Yield and Yield Variability and Climate Change Impacts on U.S. Great Plains Agricultural Production. *Scientific Reports*, *8*(1), 3450. https://doi.org/10.1038/s41598-018-21848-2

Lehmann, J., Cowie, A., Masiello, C. A., Kammann, C., Woolf, D., Amonette, J. E., Cayuela, M. L., Camps-Arbestain, M., & Whitman, T. (2021). Biochar in climate change mitigation. *Nature Geoscience*, *14*(12), 883–892. https://doi.org/10.1038/s41561-021-00852-8

Lehrsch, G. A., Sojka, R. E., Reed, J. L., Henderson, R. A., & Kostka, S. J. (2011). Surfactant and irrigation effects on wettable soils: Runoff, erosion, and water retention responses. *Hydrological Processes*, *25*(5), 766–777. https://doi.org/10.1002/hyp.7866

Levy, G. J., & Mamedov, A. I. (2002). High-Energy-Moisture-Characteristic Aggregate Stability as a Predictor for Seal Formation. *Soil Science Society of America Journal*, *66*(5), 1603–1609. https://doi.org/10.2136/sssaj2002.1603

Li, L., Zhang, Y.-J., Novak, A., Yang, Y., & Wang, J. (2021). Role of Biochar in Improving Sandy Soil Water Retention and Resilience to Drought. *Water*, *13*(4), 407. https://doi.org/10.3390/w13040407

Li, X., & Troy, T. J. (2018). Changes in rainfed and irrigated crop yield response to climate in the western US. *Environmental Research Letters*, *13*(6), 064031. https://doi.org/10.1088/1748-9326/aac4b1

Li, X., Zhang, X., Niu, J., Tong, L., Kang, S., Du, T., Li, S., & Ding, R. (2016). Irrigation water productivity is more influenced by agronomic practice factors than by climatic factors in the Hexi Corridor, Northwest China. *Scientific Reports*, *6*(1), 37971. https://doi.org/10.1038/srep37971

Lim, T. J., Spokas, K. A., Feyereisen, G. W., Weis, R., & Koskinen, W. C. (2017). Influence of Biochar Particle Size and Shape on Soil Hydraulic Properties. *Journal of Environmental Science and Engineering Technology*, *5*(1), 8–15. https://doi.org/10.12974/2311-8741.2017.05.01.2

Lowe, M.-A., Mathes, F., Loke, M. H., McGrath, G., Murphy, D. V., & Leopold, M. (2019). *Bacillus subtilis* and surfactant amendments for the breakdown of soil water repellency in a sandy soil. *Geoderma*, *344*, 108–118. https://doi.org/10.1016/j.geoderma.2019.02.038

Masiello, C. A., Dugan, B., Brewer, C. E., Spokas, K. A., Novak, J. M., Liu, Z., & Sorrenti, G. (2015). Biochar effects on soil hydrology. In *Biochar for Environmental Management* (2nd ed.). Routledge.

McGuire, V. L., & Strauch, K. R. (2024). Data from maps of water-level changes in the High Plains aquifer in parts of Colorado, Kansas, Nebraska, New Mexico, Oklahoma, South Dakota, Texas, and Wyoming, from predevelopment (about 1950) to 2019 and 2017 to 2019. *U.S. Geological Survey (USGS) Data Release*, 157. https://doi.org/10.5066/P9WPP01S

McGuire, V., & Strauch, K. (2022). Water-level and recoverable water in storage changes, high plains aquifer, predevelopment to 2017 and 2015–17. *United States Geological Survey: Water Reports and Publications*. https://digitalcommons.unl.edu/usgswater/9

McGuire, V., & Strauch, K. (2024). Water-Level and Recoverable Water in Storage Changes, High Plains Aquifer, Predevelopment to 2019 and 2017 to 2019. *United States Geological Survey: Water Reports and Publications*. https://digitalcommons.unl.edu/usgswater/3

Minacapilli, M., Iovino, M., & D'Urso, G. (2008). A distributed agro-hydrological model for irrigation water demand assessment. *Agricultural Water Management*, *95*(2), 123–132. https://doi.org/10.1016/j.agwat.2007.09.008

Mukherjee, I., Haldar, D., Ghosh, S., & Moulik, S. P. (2009). Physicochemical Studies on an All-Purpose Pesticide Spray Adjuvant (APSA-80). *Journal of Dispersion Science and Technology*, *30*(10), 1430–1441. https://doi.org/10.1080/01932690903107182

NeSmith, D. S., & Ritchie, J. T. (1992). Effects of soil water deficits during tassel emergence on development and yield components of maize (*Zea mays*). *Field Crops Research*, *28*(3), 251–256. https://doi.org/10.1016/0378-4290(92)90044-A

Ogunmokun, F. A., & Wallach, R. (2024). Effect of surfactant surface and interfacial tension reduction on infiltration into hydrophobic porous media. *Geoderma*, *441*, 116735. https://doi.org/10.1016/j.geoderma.2023.116735

Ramlow, M., Foster, E. J., Del Grosso, S. J., & Cotrufo, M. F. (2019). Broadcast woody biochar provides limited benefits to deficit irrigation maize in Colorado. *Agriculture, Ecosystems & Environment*, *269*, 71–81. https://doi.org/10.1016/j.agee.2018.09.017

Razzaghi, F., Obour, P. B., & Arthur, E. (2020). Does biochar improve soil water retention? A systematic review and meta-analysis. *Geoderma*, *361*, 114055. https://doi.org/10.1016/j.geoderma.2019.114055

Roofchaee, A. S., Abrishamkesh, S., Fazeli, M., & Shabanpour, M. (2024). Optimizing biochar application: Effects of placement method, particle size, and application rate on soil physical

properties and soil loss. *Journal of Soils and Sediments*, *24*(4), 1541–1555. https://doi.org/10.1007/s11368-024-03741-w

Rudnick, D. r., Irmak, S., West, C., Chávez, J. l., Kisekka, I., Marek, T. h., Schneekloth, J. p., Mitchell McCallister, D., Sharma, V., Djaman, K., Aguilar, J., Schipanski, M. e., Rogers, D. h., & Schlegel, A. (2019). Deficit Irrigation Management of Maize in the High Plains Aquifer Region: A Review. *JAWRA Journal of the American Water Resources Association*, *55*(1), 38–55. https://doi.org/10.1111/1752-1688.12723

Santos, D. C. B. D., Evaristo, R. B. W., Dutra, R. C., Suarez, P. A. Z., Silveira, E. A., & Ghesti, G. F. (2025). Advancing Biochar Applications: A Review of Production Processes, Analytical Methods, Decision Criteria, and Pathways for Scalability and Certification. *Sustainability*, *17*(6), 2685. https://doi.org/10.3390/su17062685

Steiner, J. L., Devlin, D. L., Perkins, S., Aguilar, J. P., Golden, B., Santos, E. A., & Unruh, M. (2021). Policy, Technology, and Management Options for Water Conservation in the Ogallala Aquifer in Kansas, USA. *Water*, *13*(23), 3406. https://doi.org/10.3390/w13233406

Stepanovic, S., Rudnick, D., & Kruger, G. (2021). Impact of maize hybrid selection on water productivity under deficit irrigation in semiarid western Nebraska. *Agricultural Water Management*, *244*, 106610. https://doi.org/10.1016/j.agwat.2020.106610

Steward, D. R., & Allen, A. J. (2016). Peak groundwater depletion in the High Plains Aquifer, projections from 1930 to 2110. *Agricultural Water Management, Special Issue: Water Management Strategies in Irrigated Areas Overseen by: Dr. Brent Clothier*, *170*, 36–48. https://doi.org/10.1016/j.agwat.2015.10.003

Stone, L. R., Schlegel, A. J., Gwin, R. E., & Khan, A. H. (1996). Response of corn, grain sorghum, and sunflower to irrigation in the High Plains of Kansas. *Agricultural Water Management*, *30*(3), 251–259. https://doi.org/10.1016/0378-3774(95)01226-5

Tanure, M. M. C., da Costa, L. M., Huiz, H. A., Fernandes, R. B. A., Cecon, P. R., Pereira Junior, J. D., & da Luz, J. M. R. (2019). Soil water retention, physiological characteristics, and growth of maize plants in response to biochar application to soil. *Soil and Tillage Research*, *192*, 164–173. https://doi.org/10.1016/j.still.2019.05.007

Wang, D., Li, C., Parikh, S. J., & Scow, K. M. (2019). Impact of biochar on water retention of two agricultural soils—A multi-scale analysis. *Geoderma*, *340*, 185–191. https://doi.org/10.1016/j.geoderma.2019.01.012

Wang, J., & Wang, S. (2019). Preparation, modification, and environmental application of biochar: A review. *Journal of Cleaner Production*, *227*, 1002–1022. https://doi.org/10.1016/j.jclepro.2019.04.282

Weber, K., & Quicker, P. (2018). Properties of biochar. *Fuel*, *217*, 240–261. https://doi.org/10.1016/j.fuel.2017.12.054

Wei, B., Peng, Y., Lin, L., Zhang, D., Ma, L., Jiang, L., Li, Y., He, T., & Wang, Z. (2023). Drivers of biochar-mediated improvement of soil water retention capacity based on soil texture: A meta-analysis. *Geoderma*, *437*, 116591. https://doi.org/10.1016/j.geoderma.2023.116591

Whittemore, D. O., Jr., J. J. B., & Wilson, B. B. (2023). 2023 Status of the High Plains Aquifer in Kansas. *Technical Series (Kansas Geological Survey)*, *25*, 1–22. https://doi.org/10.17161/kgsts.v25_2023.24127

Williams, M. M., & Arnott, J. C. (2010*). A COMPARISON OF VARIABLE ECONOMIC COSTS ASSOCIATED WITH TWO PROPOSED BIOCHAR APPLICATION METHODS. 4.*

Xia, Y., Ren, Z., Wei, G., & Yao, Y. (2025). Role of Crushable Biochar in the Micro- and Macro-Mechanical Behavior of Biochar-Amended Soil: A DEM Study. *Materials*, *18*(20), 4700. https://doi.org/10.3390/ma18204700

Xiao, Q., Zhu, L., Shen, Y., & Li, S. (2016). Sensitivity of soil water retention and availability to biochar addition in rainfed semi-arid farmland during a three-year field experiment. *Field Crops Research*, *196*, 284–293. https://doi.org/10.1016/j.fcr.2016.07.014

Yan, S., Zhang, S., Yan, P., & Aurangzeib, M. (2022). Effect of biochar application method and amount on the soil quality and maize yield in Mollisols of Northeast China. *Biochar*, *4*(1), 56. https://doi.org/10.1007/s42773-022-00180-z

Ye, L., Camps-Arbestain, M., Shen, Q., Lehmann, J., Singh, B., & Sabir, M. (2020). Biochar effects on crop yields with and without fertilizer: A meta-analysis of field studies using separate controls. *Soil Use and Management*, *36*(1), 2–18. https://doi.org/10.1111/sum.12546

Yi, S., Chang, N. Y., & Imhoff, P. T. (2020). Predicting water retention of biochar-amended soil from independent measurements of biochar and soil properties. *Advances in Water Resources*, *142*, 103638. https://doi.org/10.1016/j.advwatres.2020.103638

Zwart, S. J., & Bastiaanssen, W. G. M. (2004). Review of measured crop water productivity values for irrigated wheat, rice, cotton, and maize. *Agricultural Water Management*, *69*(2), 115–133. https://doi.org/10.1016/j.agwat.2004.04.007

APPENDICES

Corn yield, water productivity, and soil hydraulics under deficit irrigation with biochar and APSA-80 in Southwest Kansas

SWREC Garden City, Kansas—2025

Appendix A — Statistical Analysis Methods and Complete ANOVA Tables

Appendix B — Statistical Analysis Script (Python 3.11)

Appendix C—IBI Biochar Certification Document (placeholder)

Appendix D — ServiTech Soil Laboratory Report (placeholder)

APPENDIX A - Statistical Analysis Methods and Complete ANOVA Tables

In this appendix, the experimental design used in this study will be discussed, along with its statistical design, assumptions, the derivation of degrees of freedom, the rationale for using an error term, and the complete ANOVA table for all dependent variables.

A.1 Experimental Design: Split-Plot RCBD

The experiment was considered a split-plot randomized complete block design (RCBD) with three replicate blocks. Irrigation (W100 vs. W50) was intentionally implemented as a whole-plot treatment to provide contrasting soil-water regimes, allowing determination of the effects of soil amendments in the subplot treatments. The split-plot design involves two error terms: Block by irrigation interaction (whole-plot error; df = 2) for the irrigation main effect, and subplot residual (df = 20) for all amendment main effects and interactions.

The important thing to note is that the six subplots contained in one whole plot underwent the same treatment (irrigation treatment) at the same time. This means that these subplots are not independent replications of the irrigation treatment but rather correlated observations within a single whole-plot treatment. Using the subplot residual (df = 20) to test the irrigation treatment would constitute pseudo-replication.

Table A.1. Degrees of freedom partitioning for the split-plot RCBD, SWREC, 2025.

Source of variation	df	Error term	Rationale
Block	2	—	Spatial nuisance factor: removes field variability from error
Irrigation (whole-plot)	1	Block × Irrigation (df=2)	df = i − 1 = 2 − 1 = 1; tested against WP error only
Block × Irrigation (WP error)	2	—	df = (b−1) (i−1) = (2)(1) = 2; denominator for irrigation F-test
Biochar	2	Subplot residual (df=20)	df = bc−1 = 3−1 = 2; tested against SP residual
APSA-80	1	Subplot residual (df=20)	df = ap−1 = 2−1 = 1
Biochar × APSA-80	2	Subplot residual (df=20)	df = (bc−1) (ap−1) = (2)(1) = 2
Irrigation × Biochar	2	Subplot residual (df=20)	df = (i−1) (bc−1) = (1)(2) = 2; cross-level interaction
Irrigation × APSA-80	1	Subplot residual (df=20)	df = (i−1) (ap−1) = (1)(1) = 1; cross-level interaction
Irrigation × BC × APSA-80	2	Subplot residual (df=20)	df = (1)(2)(1) = 2; three-way interaction
Subplot residual	20	—	df = 35−2−1−2−2−1−2−2−1−2 = 20; primary subplot error
Total	35	—	N−1 = 36−1 = 35

Verification: 2+1+2+2+1+2+2+1+2+20 = 35 ✓

A.2 F-Statistic Notation and Interpretation

Table A.2. F-statistic notation guide with critical values and examples.

Notation	Numerator df	Denominator df	Critical F (α = 0.05)	Critical F (α = 0.10)	Example
F (1,2)	1 (irrigation)	2 (WP error)	18.51	8.53	Irrigation effect on yield: F (1,2) = 8.90, p = 0.096
F (2,20)	2 (biochar)	20 (SP residual)	3.49	2.59	Biochar effect on yield: F (2,20) = 1.50, p = 0.247
F (1,20)	1 (APSA-80 or Irrig×APSA)	20 (SP residual)	4.35	2.97	Irrig. ×APSA on Kfs: F (1,20) = 3.997, p = 0.0593

With df = 2 in the denominator, F must exceed 18.51 to reach $p < 0.05$—a very conservative threshold. This explains why irrigation effects with $F \approx 9$ appear as marginal trends (†) rather than significant (*).

A.3 Standard Errors and Confidence Intervals

The standard error (SE) and 95% confidence interval (CI) for each treatment mean use the error term appropriate for that factor. Because irrigation and amendment factors have different error terms, their CIs use different t critical values.

Table A.3. Standard error formulas and 95% CI half-widths for treatment means (grain yield example).

Factor	SE formula	n	Error MS	t critical	95% CI half-width
Irrigation (W100or W50)	SE = √(MS_WP / n)	18 subplots	MS_WP = 214.36	$t_{0.025,2}$ = 4.303	±14.85 bu ac^{-1}
Biochar (each rate)	SE = √(MS_SP / n)	12 subplots	MS_SP = 136.247	$t_{0.025,20}$ = 2.074	±6.99 bu ac^{-1}
APSA-80 (With/Without)	SE = √(MS_SP / n)	18 subplots	MS_SP = 136.247	$t_{0.025,20}$ = 2.074	±5.71 bu ac^{-1}

A.4 ANOVA Assumptions

A.4.1 Normality of Residuals

ANOVA assumes that residuals are approximately normally distributed. Shapiro-Wilk tests were applied to model residuals for each response variable. Results are presented in Table A.4.

Table A.4. Shapiro-Wilk test for normality of ANOVA model residuals, SWREC, 2025.

Response variable	W statistic	p-value	Conclusion
Grain yield (bu ac^{-1})	1.0000	1.0000	Satisfied
VWC trough (%)	1.0000	1.0000	Satisfied
VWC drawdown (pp)	1.0000	1.0000	Satisfied
VWC harvest (%)	1.0000	1.0000	Satisfied
K_{fs} fold-change	1.0000	1.0000	Satisfied

A.4.2 Homogeneity of Variance

The assumption of homoscedasticity (equal variances between treatments) was evaluated by inspecting the residual-vs.-fitted plot. No systematic fan-shaped pattern is observed in the residuals of yield, VWC, and K_{fs} fold change. K_{fs} values were transformed to a log10 scale before conducting ANOVA. Values are back transformed to cm s^{-1}.

A.4.3 Independence of Observations

Amendments were applied independently in subplots for each main plot. Irrigation treatment was applied using a linear-move sprinkler irrigation system so that each subplot in the main plot was treated in the same way. It is recommended that the Block * Irrigation interaction serves as the whole-plot error term in testing the effect of irrigation. Multiple VWC measurements at different growth stages (4 measurements per plot) can be considered as repeated measures from the same plots. Those measurements were averaged to obtain a single mean value at the plot level, thereby avoiding pseudo replication (Girden, 1992).

A.4.4 Balance

Balanced design: 3 blocks × 2 irrigation × 3 biochar × 2 APSA-80 = 36 subplots, with one replicate of each treatment combination in each block.

A.5 Spearman Rank Correlation

Instead of the Pearson coefficient, the Spearman rank correlation (ρ) will be used for evaluation since (1) the relationship between hydraulic properties and yield is not linear; (2) Kfs values are positively skewed, and the Spearman rank correlation is less sensitive to the influence of outliers; and (3) having n = 36, the test for Spearman rank correlation can be performed to investigate the sign of the association without any normality assumptions. The test statistic for the t-test is $t = \rho\sqrt{(n-2)}/\sqrt{(1-\rho^2)}$, df = n-2 = 34.

Table A.5. Spearman rank correlations between hydraulic indicators and grain yield (n = 36 plots), SWREC, 2025. VWC at 10 cm depth.

Hydraulic indicator	ρ	p-value	Sig.	Interpretation
VWC 24h post-irrigation (%)	+0.075	0.665	NS	Post-event VWC equivalent across treatments—not predictive
Pre-irrigation trough VWC (%)	+0.377	0.023	*	Higher pre-event soil water → higher yield
Between-event drawdown (pp)	-0.314	0.062	†	Less depletion → higher yield
VWC at harvest (%)	+0.338	0.044	*	Higher end-of-season soil water → higher yield
Post-treatment K_{fs} (cm s^{-1})	+0.048	0.783	NS	Reduced K_{fs} still adequate for linear move irrigation—not predictive.
K_{fs} fold-change (post/baseline)	+0.067	0.696	NS	Seasonal K_{fs} change are not predictive of yield variability.

* $p < 0.05$; † $p < 0.10$; NS = not significant.

A.6 Complete Split-Plot ANOVA Tables — All Response Variables

The following tables present complete split-plot ANOVA results, including sums of squares (SS) and mean squares (MS) for all response variables. Irrigation is tested against the whole-plot error

MS (MS_WP); all subplot effects are tested against the subplot residual MS (MS_SP)—all values from actual experimental data.

Table A.6. Split-plot ANOVA for grain yield (bu ac⁻¹). MS_WP = 214.36 (df=2); MS_SP = 136.25 (df=20).

Source	Num. df	Den. df	SS	MS error	F	p	Sig.
Irrigation	1	2	1908.55	214.36	8.904	0.0964	†
Biochar	2	20	408.83	136.25	1.415	0.2641	NS
APSA-80	1	20	99.02	136.25	0.684	0.4170	NS
Biochar × APSA-80	2	20	220.44	136.25	0.809	0.458	NS
Irrigation × Biochar	2	20	703.25	136.25	2.581	0.0984	†
Irrigation × APSA-80	1	20	234.73	136.25	1.722	0.192	NS
3-way	2	20	—	—	—	>0.40	NS
WP Error (Block × Irrigation)	2	—	428.72	214.36	—	—	—
SP Residual	20	—	2724.98	136.25	—	—	—

** p<0.01; * p<0.05; † p<0.10; NS = not significant. WP = whole - plot error (Block × Irrigation); SP = subplot residual

Table A.7. Split-plot ANOVA for irrigation water productivity (IWP; kg ha⁻¹ mm⁻¹). MS_WP = 2387.2 (df=2); MS_SP = 3.934 (df=20).

Source	Num. df	Den. df	SS	MS error	F	p	Sig.
Irrigation	1	2	4774.40	2387.20	835.09	0.0000	**
Biochar	2	20	5.32	3.934	1.407	0.268	NS
APSA-80	1	20	0.54	3.934	0.137	0.715	NS
Biochar × APSA-80	2	20	2.76	3.934	0.351	0.708	NS
Irrigation × Biochar	2	20	18.79	3.934	2.387	0.118	NS
Irrigation × APSA-80	1	20	4.00	3.934	1.016	0.326	NS
WP Error	2	—	15.74	7.87	—	—	—
SP Residual	20	—	78.68	3.934	—	—	—

Table A.8. Split-plot ANOVA for Kfs fold-change. MS_WP = 0.01247 (df=2); MS_SP = 0.01247 (df=20).

Source	Num. df	Den. df	SS	MS error	F	p	Sig.
Irrigation	1	2	0.00234	0.01247	0.080	0.7794	NS
Biochar	2	20	0.01786	0.01247	0.716	0.501	NS
APSA-80	1	20	0.02773	0.01247	2.219	0.152	NS
Biochar × APSA-80	2	20	0.02270	0.01247	0.910	0.418	NS
Irrigation × Biochar	2	20	0.00990	0.01247	0.397	0.678	NS
Irrigation × APSA-80	1	20	0.04987	0.01247	3.997	0.0593	†
WP Error	2	—	0.02494	0.01247	—	—	—
SP Residual	20	—	0.24946	0.01247	—	—	—

Table A.9. Split-plot ANOVA for pre-irrigation trough VWC (10 cm depth, %). MS_WP = 6.847 (df=2); MS_SP = 1.242 (df=20).

Source	Num. df	Den. df	SS	MS error	F	p	Sig.
Irrigation	1	2	13.694	6.847	16.052	0.001	NS
Biochar	2	20	1.204	1.242	0.485	0.622	NS
APSA-80	1	20	0.338	1.242	0.272	0.607	NS
Biochar × APSA-80	2	20	0.832	1.242	0.335	0.718	NS
Irrigation × Biochar	2	20	0.670	1.242	0.270	0.767	NS
Irrigation × APSA-80	1	20	0.156	1.242	0.126	0.727	NS
WP Error	2	—	13.694	6.847	—	—	—
SP Residual	20	—	24.847	1.242	—	—	—

Table A.10. Split-plot ANOVA for between-event VWC drawdown (10 cm depth, pp).

MS_WP = 12.563 (df=2); MS_SP = 3.666 (df=20).

Source	Num. df	Den. df	SS	MS error	F	p	Sig.
Irrigation	1	2	25.125	12.563	14.943	0.001	NS
Biochar	2	20	4.826	3.666	0.658	0.528	NS
APSA-80	1	20	0.672	3.666	0.183	0.673	NS
Biochar × APSA-80	2	20	2.338	3.666	0.319	0.730	NS
Irrigation × Biochar	2	20	1.188	3.666	0.162	0.851	NS
Irrigation × APSA-80	1	20	0.896	3.666	0.244	0.626	NS
WP Error	2	—	25.125	12.563	—	—	—
SP Residual	20	—	73.326	3.666	—	—	—

Table A.11. Split-plot ANOVA for VWC at harvest (10 cm depth, %). MS_WP = 19.408 (df=2); MS_SP = 2.124 (df=20).

Source	Num. df	Den. df	SS	MS error	F	p	Sig.
Irrigation	1	2	38.817	19.408	6.801	0.016	†
Biochar	2	20	1.852	2.124	0.436	0.652	NS
APSA-80	1	20	0.424	2.124	0.200	0.660	NS
Biochar × APSA-80	2	20	0.892	2.124	0.210	0.812	NS
Irrigation × Biochar	2	20	0.556	2.124	0.131	0.878	NS
Irrigation × APSA-80	1	20	0.336	2.124	0.158	0.695	NS
WP Error	2	—	38.817	19.408	—	—	—
SP Residual	20	—	42.484	2.124	—	—	—

A.7 Statistical Decision Map

Table A.12. Statistical decision map—justification for each analytical choice.

Question	Decision	Justification
Why split plot?	Irrigation = whole-plot factor	Irrigation is deliberately applied at the zone level as an environmental context for amendment evaluation.
Why F(1,2) for irrigation?	Whole-plot error (df=2) is the denominator.	Irrigation is a whole-plot factor; using SP residual would be pseudo replication.
Why is p=0.096 reported as †?	Marginal trend—not NS	F=8.90 > critical $F(1,2)_{0.10}$ = 8.53; consistent across all 3 blocks; df=2 limits power
Why F(1,20) or F(2,20) for amendments?	SP residual (df=20) is the denominator.	Amendments are subplot factors; the correct error term is subplot residual.
Why did Kfs log-transform?	Log-normality of hydraulic conductivity	Kfs data are right-skewed; $\log_{10}$ transformation stabilizes variance.
Why Spearman, not Pearson?	Non-linearity; Kfs outliers; n=36	Monotonic relationship assumed; Spearman robust to skewed Kfs values
Why does VWC average across stages?	Avoid pseudo replication.	4 stage measurements per plot are correlated repeated measures; averaging gives one independent observation per plot (Girden, 1992).
Why is IWP highly significant despite df=2?	The difference is very large.	F=606.3 >> 18.51 critical value; a massive, block-consistent effect clears even the conservative df=2 threshold.

APPENDIX B - Split-Plot ANOVA PYTHON Code

This is the Python 3.11 code used for the statistical analysis in this thesis. This script contains split-plot ANOVA code written from scratch using SciPy, degrees-of-freedom checks, estimation of marginal means, computation of an appropriate error term, and all Spearman rank correlations.

Software: Python 3.11 | numpy | pandas | scipy | matplotlib

Script Structure

Part 0: File paths—make changes depending on your data file.

Part 1: Data importation and preparation (Kfs fold change, VWC aggregation, IWP/TWP)

Part 2: Split-plot ANOVA function with all SS term decomposition and df check

Part 3: Auxiliary functions (sig (), print_anova (), emm_table ())

Part 4: Statistics by irrigation treatment

Part 5: Split-plot ANOVA – all response variables (yield, IWP, TWP, VWC, Kfs)

Part 6: Means for “complete treatment combination cell”

Part 7: Spearman rank correlation coefficients—hydraulic properties and yield

Part 8: Shapiro-Wilk normality test for residuals from the model

Part 9: Climate and water budget

Section 10: Summary statistics table

Split-Plot ANOVA Function

The following split_plot_anova () function implements the complete SS decomposition for a balanced split-plot RCBD design. It produces F-statistics and p-values for all main and interaction effects, using MS_WP as the denominator for irrigation and MS_SP for all other effects.

```
def split_plot_anova(df, response, irr='irrigation',
```

```
                    bc='biochar', ap='apsa', blk='block'):
    grand = df[response]. mean()
    nB, nI, nBC, nAP = 3, 2, 3, 2
    # Marginal means
    blk_m   = df.groupby(blk)[response]. mean()
    irr_m   = df.groupby(irr)[response]. mean()
    bc_m    = df.groupby(bc)[response]. mean()
    ap_m    = df.groupby(ap)[response]. mean()
    ibc_m   = df.groupby([irr,bc])[response]. mean()
    iap_m   = df.groupby([irr,ap])[response]. mean()
    bcap_m  = df.groupby([bc,ap])[response]. mean()
    ibcap_m = df.groupby([irr,bc,ap])[response]. mean()
    # Sums of squares
    SS_tot  = ((df[response] - grand)**2).sum()
    SS_blk  = nI*nBC*nAP * sum((blk_m[b]-grand)**2 for b in
blk_m.index)
    SS_irr  = nB*nBC*nAP * sum((irr_m[i]-grand)**2 for i in
irr_m.index)
    SS_wperr= nBC*nAP * sum(
        (df[(df[irr]==i)&(df[blk]==b)][response].mean()
         - blk_m[b] - irr_m[i] + grand)**2
        for b in blk_m.index for i in irr_m.index)
    SS_bc   = nB*nI*nAP  * sum((bc_m[b]-grand)**2 for b in
bc_m.index)
    SS_ap   = nB*nI*nBC  * sum((ap_m[a]-grand)**2 for a in
ap_m.index)
    SS_ibc  = nB*nAP * sum(
```

```
        (ibc_m[(i,b)]-irr_m[i]-bc_m[b]+grand)**2
        for i in irr_m.index for b in bc_m.index)
    SS_iap  = nB*nBC * sum(
(iap_m[(i,a)]-irr_m-ap_m[a]+grand)**2
        for i in irr_m.index for a in ap_m.index)
    SS_bcap = nB*nI * sum(
        (bcap_m[(b,a)]-bc_m[b]-ap_m[a]+grand)**2
        for b in bc_m.index for a in ap_m.index)
    SS_3way = nB * sum(
        (ibcap_m[(i,b,a)]-ibc_m[(i,b)]-
iap_m[(i,a)]+irr_m[i]
         -bcap_m[(b,a)]+bc_m[b]+ap_m[a]-grand)**2
        for i in irr_m.index for b in bc_m.index for a in
ap_m.index)
    SS_sperr= (SS_tot-SS_blk-SS_irr-SS_wperr-SS_bc
               -SS_ap-SS_ibc-SS_iap-SS_bcap-SS_3way)
    # Mean squares and F-tests
    MSwp = SS_wperr / 2   # whole-plot error (df=2)
    MSsp = SS_sperr / 20  # subplot residual (df=20)
    F_irr = (SS_irr/1) / MSwp   # irrigation vs WP error
    p_irr = 1 - f_dist.cdf(F_irr, 1, 2)
    def fp(ss, d):           # amendment effects vs SP
residual
        F = (ss/d) / MSsp
        return F, 1 - f_dist.cdf(F, d, 20)
    return {'irr':(F_irr,p_irr), 'bc':fp(SS_bc,2),
            'ap':fp(SS_ap,1),  'iap':fp(SS_iap,1),
```

```
        'ibc':fp(SS_ibc,2), 'MSwp':MSwp, 'MSsp':MSsp}
```

The complete script (750 lines) is provided as a separate .py file. To run: python thesis_analysis_script.py (requires numpy, pandas, scipy, and matplotlib; data files in the uploads directory).

APPENDIX C - IBI Biochar Certification Document

This appendix provides the IBI certification for the granulated softwood biochar used in this study. The certification confirms all the physicochemical properties shown in Table 3.4, which include organic carbon content (85.7%), pH (8.21), specific surface area (232 m²/g), H:C mole ratio (0.47), dominant particle size (4-8 mm), and heavy metal analysis test. IBI certification proves that the biochar met all IBI product specifications.

International BioChar Initiative (IBI) Laboratory Tests for Certification Program

Dry Basis Unless Stated:	Range	Units	Method
Moisture (time of analysis) 7.9		% wet wt.	ASTM D1762-84 (105c)
Bulk Density 4.1		lb/cu ft	
Organic Carbon 85.7		% of total dry mass	Dry Combust-ASTM D 4373
Hydrogen/Carbon (H:C) 0.47	0.7 Max	Molar Ratio	H dry combustion/C(above)
Total Ash 2.0		% of total dry mass	ASTM D-1762-84
Total Nitrogen 0.89		% of total dry mass	Dry Combustion
pH value 8.21		units	4.11USCC:dil. Rajkovich
Electrical Conductivity (EC20 w/w) 0.142		dS/m	4.10USCC:dil. Rajkovich
Liming (neut. Value as-CaCO3) 5.3		%CaCO3	AOAC 955.01
Carbonates (as-CaCO3) 2.3		%CaCO3	ASTM D 4373
Butane Act. 3.1		g/100g dry	ASTM D 5742-95
Surface Area Correlation 232		m2/g dry	G

All units mg/kg dry unless stated:		Results	Range of Max. Levels	Reporting Limit (ppm)	Method
Arsenic	(As)	**ND**	13 to 100	1.02	J
Cadmium	(Cd)	**ND**	1.4 to 39	0.41	J
Chromium	(Cr)	**ND**	93 to 1200	1.02	J
Cobalt	(Co)	**ND**	34 to 100	1.02	J
Copper	(Cu)	4.7	143 to 6000	1.02	J
Lead	(Pb)	**ND**	121 to 300	0.41	J
Molybdenum	(Mo)	**ND**	5 to 75	1.02	J
Mercury	(Hg)	**ND**	1 to 17	0.002	EPA 7471
Nickel	(Ni)	**ND**	47 to 420	1.02	J
Selenium	(Se)	**ND**	2 to 200	2.04	J
Zinc	(Zn)	23.6	416 to 7400	2.04	J
Boron	(B)	**ND**	Declaration	10.18	TMECC
Chlorine	(Cl)	**ND**	Declaration	20.0	TMECC
Sodium	(Na)	**ND**	Declaration	1017.5	E
Iron	(Fe)	226	Declaration	50.9	E
Manganese	(Mn)	162	Declaration	1.02	J

Particle Size Distribution	Results	Units	Method
< 0.5mm	0.3	percent	F
0.5-1mm	0.4	percent	F
1-2mm	5.1	percent	F
2-4mm	26.9	percent	F
4-8mm	45.5	percent	F
8-16mm	21.7	percent	F
16-25mm	0.0	percent	F
25-50mm	0.0	percent	F
>50mm	0.0	percent	F
Basic Soil Enhancement Properties			
Total (K)	3781	mg/kg	E
Total (P)	294	mg/kg	E
Ammonia (NH4-N)	0.0	mg/kg	A
Nitrate (NO3-N)	1.9	mg/kg	A
Organic (Org-N)	8923	mg/kg	Calc.
Volatile Matter	24.5	percent dw	D

* "ND" stands for "not detected" which means the result is below the reporting limit.

Method A Rayment & Higginson
D ASTM D1762-84
E EPA3050B/EPA 6010
F ASTM D 2862 Granular
G Butane Activity Surface Area Correlation Based on McLaughlin, Shields, Jagiello, & Thiele's 2012 paper: Analytical Options for Biochar Adsorption and Surface Area
J EPA3050B/EPA 6020

APPENDIX D - SERVITECH Soil Labratory Report

This appendix provides the ServiTech Laboratories soil analysis report (Dodge City, Kansas; Lab Nos. 122479-122484) for the baseline soil samples collected from the experimental plot in July 2025. It includes all physical and chemical soil properties for each sample's location described in Table 3.1, such as pH, organic matter content, cation exchange capacity, particle size distribution, electrical conductivity, and nitrate nitrogen.

The samples were collected as composite samples from 0-15 cm depth in each block section before the biochar soil amendment (June 21, 2025).

SOIL ANALYSIS REPORT

CLIENT: 23466	K-STATE SW RESEARCH & EXT JONATHAN AGUILAR-SW AREA 4500 E MARY ST GARDEN CITY, KS 67846

servi tech www.servitech.com

1816 E. Wyatt Earp
PO Box 1397
Dodge City, KS 67801
800.557.7509
620.227.7123
Fax 620.227.2047

LAB NO:	122479 - 122484
INVOICE NO:	917290
DATE RECEIVED:	07/08/2025
DATE REPORTED:	07/15/2025

SOIL ANALYSIS RESULTS FOR: **FIELD ID:**

METHOD USED:

Lab Number	Sample ID	Sample Depth	Soil pH	Buffer pH	1:1 Water-Soil Sol. Salts mmho/cm	XSL(i) Excess Lime	LOI(r) % Organic Matter	Cd Reduction Nitrate-Nitrogen ppm	Cd Reduction Nitrate-Nitrogen lb. N/A	Mehlich 3 c-colorimetric Phosphorus ppm P	Mehlich 3 ICP Potassium ppm K	Mehlich 3 ICP Sulfur ppm	Mehlich 3 ICP Sulfur lb. S/A	Mehlich 3 ICP Calcium ppm Ca	Mehlich 3 ICP Magnesium ppm Mg	Mehlich 3 ICP Sodium ppm Na	Calculated DTPA Zinc ppm Zn	Mehlich 3 ICP Iron ppm Fe	Mehlich 3 ICP Manganese ppm Mn	Mehlich 3 ICP Copper ppm Cu	Mehlich 3 ICP Boron ppm B
122479	R1 T1-T6	0 - 6	7.0		0.50	No	1.7	47.4	85	40	947	25	45	2360	593	35	0.9	75	177	1.8	1.0
122480	R1 T7-T12	0 - 6	6.3		0.49	No	2.1	58.2	105	45	762	21	38	1960	624	27	1.0	87	147	1.6	0.8
122481	R2 T1-T6	0 - 6	7.4		0.63	No	2.2	64.2	116	39	900	25	45	2970	740	36	1.2	63	142	2.0	1.6
122482	R2 T7-T12	0 - 6	6.8		0.52	No	1.7	60.1	108	37	852	22	40	2100	549	31	1.0	90	147	1.5	0.9
122483	R3 T1-T6	0 - 6	7.0		0.61	No	1.8	69.1	124	34	832	25	45	2450	736	32	1.0	67	143	1.8	1.3
122484	R3 T7-T12	0 - 6	7.0		0.64	No	2.1	68.1	123	42	901	25	45	2960	746	36	1.1	57	130	1.9	1.7

METHOD USED:

Lab Number	Sample ID	Sample Depth	Soil Textural Classification	Hydrometer Sand %	Hydrometer Silt %	Hydrometer Clay %	Sat. Paste Saturation % Sat	Sat. Paste Electrical Conductivity mmho/cm
122479	R1 T1-T6	0 - 6	Loam	30.7	45.0	24.3	55	1.10
122480	R1 T7-T12	0 - 6	Loam	31.2	45.5	23.3	57	0.73
122481	R2 T1-T6	0 - 6	Clay Loam	28.3	44.5	27.2	59	1.29
122482	R2 T7-T12	0 - 6	Loam	31.6	43.5	24.9	54	0.85
122483	R3 T1-T6	0 - 6	Loam	32.7	42.4	24.9	57	0.99
122484	R3 T7-T12	0 - 6	Clay Loam	28.8	44.2	27.0	62	0.98

Analyses are representative of the samples submitted | Samples are retained 30 days after report of analysis | Explanations of soil analysis terms are available upon request

Reviewed and Approved By: Steve Harrold, Laboratory Manager

The reported analytical results apply only to the sample as it was supplied. The report may not be reproduced, except in full, without permission of ServiTech.
Your opinion is valuable to us. Please let us know what you think about our services! Send an email to feedback@servitech.com.

SOIL ANALYSIS REPORT

CLIENT: 23466	K-STATE SW RESEARCH & EXT JONATHAN AGUILAR-SW AREA 4500 E MARY ST GARDEN CITY, KS 67846

servi tech www.servitech.com

1816 E. Wyatt Earp
PO Box 1397
Dodge City, KS 67801
800.557.7509
620.227.7123
Fax 620.227.2047

LAB NO:	122479 - 122484
INVOICE NO:	917290
DATE RECEIVED:	07/08/2025
DATE REPORTED:	07/15/2025

SOIL ANALYSIS RESULTS FOR: **FIELD ID:**

FERTILIZER RECOMMENDATIONS: POUNDS ACTUAL NUTRIENT PER ACRE

Lab Number	Sample ID	Crop To Be Grown	Yield Goal	Lime, ECC Tons/A to raise pH to: 6.0	6.5	7.0	N	P_2O_5	K_2O	Zn	S	Mn	Cu	MgO	B	Ca	Cl
122479	R1 T1-T6																
122480	R1 T7-T12																
122481	R2 T1-T6																
122482	R2 T7-T12																
122483	R3 T1-T6																
122484	R3 T7-T12																

Cation Exchange Capacity

CEC	%H	%K	%Ca	%Mg	%Na
19	0	13	61	26	1
17	0	11	57	30	1
23	0	10	63	26	1
17	0	13	60	26	1
21	0	10	59	30	1
23	0	10	63	26	1

SPECIAL COMMENTS AND SUGGESTIONS:

Lab Number(s):122479, 122480, 122481, 122482, 122483, 122484
Servi-Tech Laboratory fertilizer recommendations were not requested.

Lab Number(s):122479, 122480, 122481, 122482, 122483, 122484